

EEG based BCI: measurement and quality control

Wesmond Lee & Thibault Los

Delft University of Technology



EEG based BCI: measurement and quality control

by

Wesmond Lee & Thibault Los

to obtain the degree of Bachelor of Science
at the Delft University of Technology,
to be defended publicly on 29 June at 11:00 AM.

Project duration: April 24, 2023 – June 15, 2023
Thesis committee: Prof. dr. B. Hunyadi, TU Delft, supervisor
Prof. dr. ir. L. Abelmann, TU Delft
Prof. dr. A. Cardoso, TU Delft

An electronic version of this thesis is available at <http://repository.tudelft.nl/>.

Abstract

Purpose

The main purpose of this report is to find out whether the OpenBCI "Ultracortex Mark IV" Electroencephalogram (EEG) headset is capable of differentiating EEG-signals of motor execution from neutral state with recorded data and to find out whether it can differ motor executions between left and right hand. Next to that, it is to be determined whether the OpenBCI headset was the optimal one for this purpose.

Method

First, the specifications of different headsets were compared. Afterwards, a montage of the electrodes was designed to detect motor execution and motor imagery, mainly centered around the locations C3, Cz and C4, on the top of the scalp. The software "Openvibe" was used to extract data from the headset during experiments and to record it in a csv file. A subject was asked to follow a video with a sound cue followed by a visual cue instructing to move either its left hand or right hand.

Result

Merging the left and right hand trial data together, the result is that the headset shows in the alpha band (7-12 Hz) mostly a decrease (ERD) in magnitude around the visual cue, sometimes followed by a bigger increase in magnitude (ERS). Looking at the extremes after the cue, it is seen that mostly the difference in magnitude is around a factor 1.5 compared to the average magnitude of before the visual cue. Splitting the trial data between left and right hand, similar results can be seen, but one hand produces slightly more ERD or ERS than the other hand depending on the position of the electrode on the left or right hemisphere of the brain.

Conclusion

The OpenBCI headset can in fact detect a difference between movement of the hands and the neutral state. Differentiating between the movements of left and right hands seems possible from the results, but the difference in the signal of left and right hand is minimal. It is recommended to repeat the experiment with more trials and different subjects to get a more solid conclusion.

Preface

This thesis is written in context of the Bachelor Graduation Project. The goal of the overall project was to design a brain computer interface (BCI) to play a game using motor imagery. During the project it was found that this was probably too difficult, and it was decided to focus on playing a game using motor control. To achieve this, different measurements were done and analysed. The total group consists of six people which is divided into three subgroups. This thesis will focus on the measurement and quality control part of the project. We would like to express our gratitude to our daily supervisor prof. dr. Borbála Hunyadi. Additionally we want to thank Seline de Rooij, Sofia Kotti and Ruben Wijnands for their assistance. We are very thankful to prof.dr.ir Leon Abelman for his help during the project. Thirdly we are grateful to ing. Martin Schumacher, who played the role of test-subject for numerous tests throughout the project. Finally we want to thank our colleagues: Joris van de Weg, Marlon van Zijl, Anthony Dai and Chelsea Apawti. We hope that this project will be picked up and further developed after completion of this thesis, since it is a interesting subject.

*Wesmond Lee & Thibault Los
Delft, July 2023*

Contents

1	Introduction	1
2	Program of Requirements	2
3	Hardware overview	4
3.1	Requirements headset	4
3.1.1	Types of electrodes	5
3.2	Comparison selected headsets	5
3.3	OpenBCI headset	6
4	Data acquisition	8
4.1	Montage	8
4.2	Software	11
4.3	Pre-processing	13
4.4	Paradigms	14
5	Data analysis	15
5.1	Background	15
5.2	Pre-processing	16
5.3	Measurements	17
5.3.1	Blinking	17
5.3.2	Motor execution	18
5.3.3	Motor imagery	21
5.4	Quality improvement	22
5.4.1	Human antenna	22
5.4.2	Pre-cautions	22
5.4.3	Noise reduction	22
5.5	Consistency	24
5.5.1	Focus	24
5.5.2	Subject differences	25
6	Conclusion and discussion	26
6.1	Conclusion	26
6.2	Discussion	27
	References	29
A	Additional figures hardware overview	32
A.1	OpenBCI electrodes	32
B	Additional figures data acquisition	33
B.1	Brain structure	33
B.2	Overview methodologies	34
B.3	OpenVibe scenario	35
B.4	Pre-processing filters	36
B.5	OpenBCI GUI	37
C	Additional figures data analysis	38
C.1	Raw signal	38
C.2	PSD plots	39
C.3	Window sizes	40
C.4	Average magnitude plots	41
C.5	Beta band magnitude plots	42

- C.6 Quality improvement 43
 - C.6.1 Human antenna 43
 - C.6.2 Noise reduction 43

1

Introduction

This paper is part of a project to design a brain computer interface (BCI) to play a game on a computer using an EEG headset in real-time. The project is divided into three subgroups: measurement and quality control, decoding and interface subgroup. This paper will present the work of the measurement and quality control subgroup, which is responsible for measuring and pre-processing EEG signals with an EEG headset and send the acquired data to the decoding group. The decode group will then decode the EEG signals, using a trained model, to a command to be used for the game created by the interface group.

As described earlier, this project will make use of a BCI. Brain Computer Interface (BCI) is a popular research topic for scientists and researchers. A BCI is a system that decodes brain waves into a command to be used in an external program, such as a game. A popular technique to record brain signals is the Electroencephalogram (EEG). In recent years many wireless portable EEG devices have been developed that cost less than €5000, which gives individuals more opportunity to work with EEG data. The devices are non-invasive and small enough to be easily portable; this makes EEG a more attractive option compared to other methods like MEG which is non-portable [22].

Several artifacts can cause disturbance to EEG recordings such as motion artifacts, heart rhythms, eye movements and muscle activity. Artifacts from muscles will probably be easy to filter as they are most concentrated between 30 and 100 Hz[5]. However, it is more difficult to deal with motion artifacts as they can easily occur and are difficult to filter out since they do not have a specific frequency. Eye blinks however, will most probably not give a significant artifact as they will influence the signal for only a short amount of time.

Based on the program of requirements, it will be decided which of the two available headsets, the OpenBCI Ultracortex Mark IV and the Neurosky Mindwave, will be used during the project. Additionally it will be decided which application will be used to extract and process the data from the chosen headset. Multiple experiments will be conducted to decide if the data is high enough quality to be able to distinguish different classes. The quality of the EEG signals will be determined by analysis tools like a spectrogram and the power spectral density (PSD).

2

Program of Requirements

The program of requirements is set to clearly state what the deliverables and goals of the measurement and quality control group are. The main goal of the measurement and quality control subgroup is to measure and pre-process EEG signals with an EEG headset. The requirements are divided into must and should requirements. The must requirements are mandatory as these are needed to successfully accomplish the goal of the measurement and quality control subgroup. The should requirements are set in such way that it would be nice if these requirements are met and are needed to successfully integrate the whole project, but will not contribute to the goal of the subgroup. If all requirements (including the should requirements) are met, it will be possible to live-stream high quality motor imagery data to the decode subgroup to decode the signals into a command using a training model. This model needs to be trained with measured data. The must and should requirements for the measurement and quality control subgroup are:

Must requirements:

- The own measurements must:
 - Detect EEG of blinking; the measurements in time domain must show an amplitude difference of at least a factor 10 on average between a blink and no blink.
 - Have at least 2 classes (rest and movement of both hands) must be distinguished in a EEG recording in frequency domain; the measurements must show a magnitude difference of at least factor 1.5 on average in the alpha band (7 - 12 Hz) during a motor execution compared to neutral position.
 - Have at least 50 trials of motor execution of both left and right hand to gain test and training data for the decoding group.
- The must requirements set for the headset are:
 - The electrodes of the chosen headset must be able to be placed at the areas to measure the EEG signals of: blinking, motor execution and motor imagery.
 - Headset cost must be under €5000.
 - A sampling frequency of at least 60 Hz.
- The must requirements set for the acquisition software are:
 - The used acquisition software must have at least support for the OpenBCI "Ultracortex Mark IV" and Neurosky "Mindwave MW001" headset.
 - The used acquisition software must be able to record the output of the headset and save a sample of minimum two minutes into a csv file.

Should requirements:

- Own measurement should satisfy:
 - At least 2 classes (rest and imagery movement of both hands) must be distinguished in a EEG recording in frequency domain; The measurements must show a magnitude difference of at least factor 1.5 in the alpha band (7 - 12 Hz) during a motor imagery compared to neutral.
 - At least 25 trials of motor imagery from left and right hand to gain test and training data for the decoding subgroup.
 - At least 3 classes (left hand, right hand and rest) must be distinguished during the recording; the measurements must show a magnitude difference of at least a factor 1.5 on average in the alpha band (7 - 12 Hz) during a motor execution compared to neutral and the other hand.
- The should requirements set for the headset are:
 - The location of the electrodes can be variably placed according to the 10-20 system [13].
 - Headset cost should be as low as possible while complying with all the must requirements.
- The should requirements set for the acquisition software are:
 - Be able to live-stream data to the decoding group.
 - Should have support for (at least 10) different headsets, including the OpenBCI and Neurosky Mindwave headset.

3

Hardware overview

This chapter will focus on the hardware that is used during the project which will consist of the EEG headset. This chapter will decide, based on the set requirements, which headset is most suitable and will explain the working of the selected headset.

3.1. Requirements headset

Recording the brain activity is the first step in controlling a game using brain activity. Invasive neural signals have a high spatial resolution, but has a high safety risk as the sensor, which has to be implanted can cause immune response and callus after surgery. Non-invasive neural signals are safer than invasive neural signals as they can provide an interface without surgery. To record the brain signals an popular technique is the Electroencephalogram (EEG). EEG provides a descent time resolution, is non-invasive and is portable compared to other methods [22]. An EEG system is composed of a cap on which the electrodes are placed, a signal amplifier and an analog-to-digital (A/D) converter. The signal amplifier is needed as the signals from the brain have naturally a low amplitude. The A/D converter is needed to convert the analog brain signals to digital signals, which can be read out digitally. This digital signal can for instance be processed by a personal computer.

Before it is possible to select a headset to measure EEG signals, the requirements for the headset have to be set. The must requirements that have been set for the headset are:

- The electrodes of the headset must be placed at the areas to measure the EEG signals of: blinking, motor execution and motor imagery.
- Price must be below €5000
- A sampling frequency of at least 60 Hz.

One of the most important requirements is that the headset can measure blinking, motor execution and motor imagery. To fulfill this requirement, the headset must have electrodes on specific places on the head. For detecting blinking the headset must have electrodes on either location Fp1 or Fp2 [2] according to the 10-20 system [13]. For motor execution and motor imagery the electrodes needs to be placed close to the motor cortex area. The locations of the 10-20 system that correspond with this are C3,C4,Cz, P3 and P4. More about the montage of the headset will be described in section 4.1. The requirement of the locations for measuring eye blinks is set so that it is probably easier for the decode group to filter out unwanted eye blinks. Also, if it occurs that detecting motor execution or motor imagery is not possible, detecting eye blinks could be a good alternative. One aspect to also take into account is the price of the headset. The upper limit for the price of the headset is set to €5000. The last requirement is that the headset must have a sampling frequency of at least 60 Hz. This is set because the EEG signals of motor execution and motor imagery will be between 7 and 30 Hz [15] [14], so the highest frequency that the headset is required to measure is 30 Hz. If Nyquist is taken into account, this will lead to a minimum required sampling frequency of 60 Hz.

Beside the must requirements, there are also two should requirements set for the headset: the location of the electrodes can be variably placed according to the 10-20 system and the price of the headset

should be as low as possible. The first should requirement is set to give the opportunity to place the electrodes on the best places to meet the must requirements if the default layout on the headset is not suitable for that. The second requirement is set to minimize the cost of the headset.

3.1.1. Types of electrodes

There are roughly two kind of electrodes: dry and wet electrodes. Both types have there own advantages and disadvantages which will be discussed below.

Wet electrodes are commonly made of silver with a coating of silver chloride (Ag/AgCl). Additionally, a gel containing chloride ions is applied between the electrode and the skin. This improves the conduction and reduces the skin-electrode interface impedance. Adding this gel requires extra preparation time as the electrodes need to be cleaned and dried. This gel will also give some inconvenience for the subject as their hair needs to be cleaned. To improve the conductivity of wet electrodes, the skin needs to be slightly scratched which can feel uncomfortable. Wet electrodes are commonly wire-connected. The advantage of wet electrodes is that they can ensure a higher signal quality compared to dry electrodes. This is also due to the fact that wet electrodes are less susceptible to mains interference and movement artifacts than dry electrodes.

Dry electrodes were proposed to overcome the issues with the gel of wet electrodes. Dry electrodes consist of a conductive material that couples with the skin. These electrodes could consist of different kind of materials. The most significant disadvantage of dry electrodes is that the impedance of the electrode is higher compared to that of wet electrodes. This increase in impedance can lead to poor contact with the scalp, increased instability and more let the electrodes be more sensitive to noise. One of the biggest advantages of dry electrodes is the quicker setup time compared to wet electrodes.

Research found that the impedance for dry electrodes is slightly higher compared to wet electrodes. However, the resting state EEG power and event-related potentials were comparable between the two types. The same research found that dry electrodes are more robust to 50 Hz line noise and other electromagnetic interference from ambient noise [10]. Another study found that dry electrodes guarantee the same amount of quality as wet electrodes [7]. As previous studies stated, there is almost no benefit to using wet electrodes compared to dry electrodes. As a consequence, it was decided to use dry electrodes during this project.

3.2. Comparison selected headsets

As stated in the previous section, it was decided to use dry electrodes. As a consequence of this, only headsets which contain dry electrodes will be used in this project. There are different requirements set for the headset, such as possibility to measure eye blinks, motor imagery, price and minimum sampling frequency. Two EEG headsets are available for this project: the OpenBCI "Ultracortex Mark IV" and the Neurosky "Mindwave MW001". For completeness, two other commonly available EEG headsets are included in the comparison as well: the InterAxon Muse 2 and the Emotiv EPOC. Table 3.1 shows a comparison of the properties of the different headsets.

The OpenBCI Ultracortex Mark IV is an open-source 3d printable headset. The headset is standard equipped with 8 electrodes, which can be extended to 16 using the available extension board. The skeleton is 3d printed and contains 35 different locations based on the 10-20 international system to place the electrodes. The OpenBCI headset requires assembly prior to use. As the electrodes of the OpenBCI headset can be flexibly placed along 35 locations, detecting the EEG signals of eye blinks, motor imagery and motor execution is possible. The main disadvantage of the OpenBCI headset is the price, which is higher compared to the other headsets. The OpenBCI headset has a ground and reference node which are placed at both earlobes of the subject.

The Neurosky "Mindwave MW001" headset is a single-channel low-cost headset. The headset is the cheapest headset with a price around €200. The headset has only 1 electrode which is placed at the forehead of the subject. The placement of this electrode is limited adjustable. With a sampling frequency of 512 Hz, this headset has one of the highest sampling frequencies. As the electrode is only located on the forehead, it is not possible to detect motor imagery or motor execution. The Neurosky headset contains of two reference nodes, one at the left earlobe (A1 location) and one on location T4.

Properties	OpenBCI Ultracortex "Mark IV"	Neurosky "Mindwave MW001"	InterAxon "Muse 2"	Emotiv "EpoC"
Number of electrodes	8 (can be extended to 16)	1	4	14
Placing electrodes (according to 10-20 system)	35 locations	Fp1	AF7, AF8, TP9 and TP10	AF3,F7,F3,FC5, T7,P7,O1,O2,P8, T8,FC6,F4,F8 and AF4
Sampling frequency	250 Hz	512 Hz	256 Hz	128 or 256 Hz
Communication	Bluetooth	Bluetooth	Bluetooth	Bluetooth
Potential to detect eye blinks	yes	yes	yes	yes
Potential to detect motor imagery	yes	no	no	yes
Results on web of science ¹	82	137	17	425
Cost	€2600	€200	€400	€850

Table 3.1: Comparison different EEG headsets [16]

InterAxon offers the muse 2, which contains 4 electrodes. These electrodes have fixed locations. It should be possible to detect eye blinks with it, but no motor imagery or motor execution. The sampling frequency is with 256 Hz lower than that of the Neurosky. The Interaxon muse 2 has the lowest results on Web of Science which implicates that the headset has probably been used prior in less projects. The Interaxon muse 2 contains of 3 reference nodes which are all placed on the forehead of the subject, The Emotiv EpoC contains 14 electrons which were placed on different positions. The positions of these electrodes are limited adjustable. The headset has two reference nodes at location P3 and P4. The Emotiv EpoC headset has the most results on Web of Science of all headsets which implies that there are probably more research projects already done with this headset.

All headsets are communicating with the computer using Bluetooth. Looking at the requirements that were set for the headset, one of the requirements was that it is possible to detect motor imagery and motor execution. Looking at the comparison, only the OpenBCI and the Emotiv will meet this requirement. The difference between these two headsets is the number of electrodes and the placing of the electrodes. Although the OpenBCI headset is the most expensive headset, it is decided for this project that the OpenBCI headset is the most optimal. The main reason is the flexible placement of the electrodes. This way the electrodes could be placed in the locations which are the most important for measuring motor imagery. Besides that, OpenBCI offers a detailed documentation about their product.

3.3. OpenBCI headset

The OpenBCI Ultracortex "Mark IV" headset can be divided into three components: the frame with the electrodes, the processing module and the USB module.

The frame (Figure 3.1) is a 3d printed frame with 35 locations for electrodes. These locations are based on the 10-20 international system. The layout of electrode locations of the headset can be found in Figure 4.2b. There are two different dry electrodes available: a spikey one, which can be used in hair, and a non spikey one, which can be used for nodes with no hair (like the forehead). The non spikey electrodes are commonly placed at Fp1 and Fp2. Besides using these electrodes, it is also possible to use so-called comfort units, which are similar to electrodes. The function of these comfort units is to distribute the weight of the headset over the head of the subject to get a more comfortable feeling. These units are not connected to the processing unit. The two kind of electrodes and the comfort units can be found in Figure A.1. During the different experiments it was found that the spikey electrodes can feel uncomfortable for some subjects. This is due to the fact that the electrodes have to make

¹<https://www-webofscience-com.tudelft.idm.oclc.org/wos/woscc/basic-search>

contact with the skin, which can be uncomfortable when using the spikey electrodes. A subject with less hair will not or less experience this issue. More information about the used montage can be found in section 4.1.

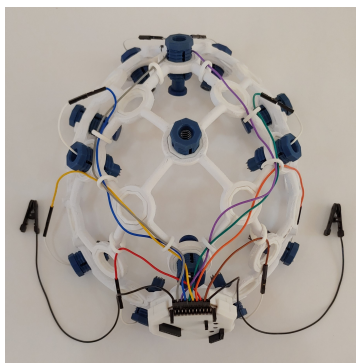


Figure 3.1: The OpenBCI ultracortex IV

All electrodes are wire-connected on the processing module. The standard connected board is the OpenBCI Cyton board, which can handle up to 8 channels. Beside the 8 channels, the board contains also a reference and a bias signal, which can be placed using clips on for example the earlobes. The board contains the PIC32MX250F128B microcontroller [21]. The incoming data is sampled at 250 Hz on each of the eight channels. The board is compatible with passive and active electrodes. Beside that, the board contains an analog to digital converter (ADC), which is in this case the Texas Instruments ADS1299 ADC [11]. It also contains 3 accelerometers to measure the movement of the head; the LIS3DH accelerometer is used for this. The gain of the board is programmable to the following values: 1, 2, 4, 6, 8, 12 or 24. The Cyton board uses Bluetooth to communicate with the USB dongle. The USB dongle establishes the connection using Bluetooth with the Cyton module. The USB dongle establishes the connection between the headset and the PC. The USB module contains the radio transceiver RFD22301 [6] for the Bluetooth low energy connection. The data is recorded using a 24 bit resolution. The data is saved following the format: timestamp, 8 channels EEG, 3 accelerometer channels [25]. This data can be further processed by a computer by reading out the serial port.

4

Data acquisition

This chapter will focus on extracting data from the chosen OpenBCI Ultracortex "Mark IV" EEG Headset to differentiate the brain signals for motor imagery/control. To do so, there are multiple factors to take into account, such as: the montage of electrodes on the human scalp, the software to decipher the received signals from the headset, the pre-processing of the signals and the methodology of experiments to ensure a as consistent acquirement of reliable data possible.

4.1. Montage

One of the first factors to take into account is the correct placement of the electrodes on the scalp. In this project, the headset should receive motor control/imagery signals from the brain. To do so, one must first know what regions of the brain has the most activity when a person moves or wants to move a certain part of the body.

It was found that most of the signals for the motor functionality of a body were generated in the brain area called the "motor cortex" which lays near the frontal lobe of the brain (Figure B.1). This corresponds mostly with the meta-analysis of Hardwick(2017)[8] on active regions during motor imagery and motor execution, albeit the meta-analysis also showed some activity in the parietal lobes.

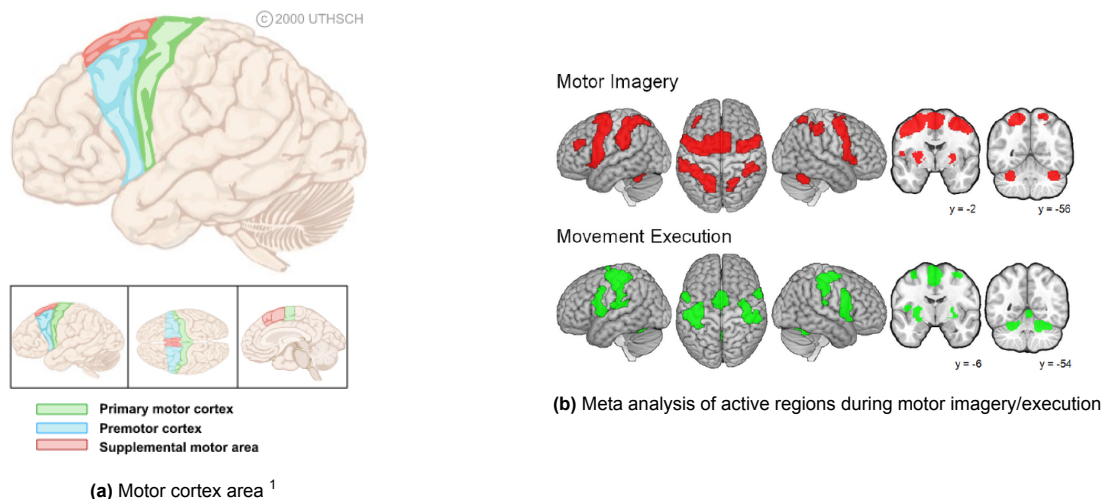
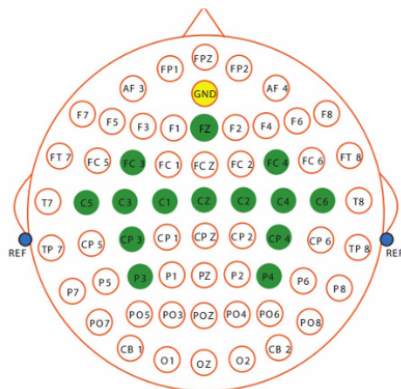


Figure 4.1: Figures of the motor cortex and Meta analysis of active regions during motor imagery/execution

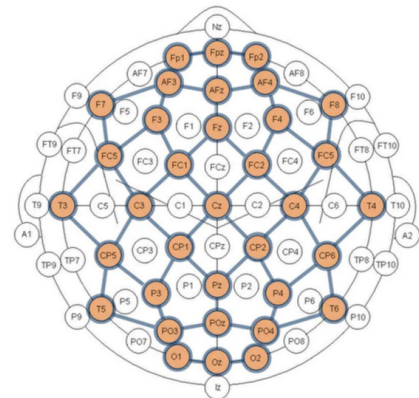
With this knowledge, a correct placement of the electrodes could be derived. Looking at the commonly used 10-20 system for the placement of the electrodes, it was hypothesised that the most important areas to place the electrodes and detect motor imagery/execution signals would be around the locations

¹<https://nba.uth.tmc.edu/neuroscience/m/s3/chapter03.html>

C3, C4 and Cz. Looking into the montages of papers which also conducted motor imagery experiments, such as Zhang(2019)[34] our theory was highly plausible.



(a) Montage of Zhang(2019) [34]



(b) Electrode layout of OpenBCI Ultracortex Mark IV headset (In orange)²

Figure 4.2: Figures of the montage of Zhang(2019) and the layout of the OpenBCI Ultracortex Mark IV headset

Table 4.1: 8 electrode configuration

Channel	Position
1	Fp1
2	Fp2
3	Fz
4	Cz
5	C3
6	C4
7	P3
8	P4

Table 4.2: 16 electrode configuration

Channel	Position	Channel	Position
1	Fp1	9	Cz
2	Fp2	10	C4
3	Fz	11	Cp5
4	Fc5	12	Cp1
5	Fc1	13	Cp2
6	Fc2	14	Cp6
7	Fc6	15	P3
8	C3	16	P4

Unfortunately, it was not possible to exactly replicate the existing montages since the OpenBCI headset only supported a limited amount of pre-determined places to screw new electrodes into. Due to this limitation, from the 8 electrodes, it was decided to place the 6 most important electrodes on Fz, Cz, C3, C4, P3 and P4 as shown in table Table 4.1. The other 2 electrodes were placed on Fp1 and Fp2, for the eyeblink detection that the decoding subgroup might need for their artefact removal algorithm or in case that the motor imagery/execution signal received from the brain is not of high enough quality and eye blinking has to be used to control the computer interface.

Initially, it was thought of to extend the amount of electrodes used from 8 to 16 and place them like described in table Table 4.2. This way, an increased area of the motor cortex and parietal lobes can be measured and can the activity during motor activities better be localized. Eventually, it was chosen not to take measurements for training data with it due to the following reasons:

- With 8 electrodes, it could already be seen that sometimes the contacts of around 2 electrodes would fail to reach the scalp due to the thickness and length of a test person its hair. This could be fixed most of the time by brushing away the hair of said test person at the spot of the failing electrode and adjusting the depth of which the electrode is screwed into the headset. With 16 electrodes, the amount of failing electrodes rose to 3-4 electrodes most of the time and to solve the issue for every other test person is not worth the time investment.
- Next to that, due to the layout of the OpenBCI headset, 8 electrodes already cover the most important places around the C3 and C4 areas. With 16 electrodes, it is possible to fill T7, CP5,

²<https://shop.openbci.com/products/ultracortex-mark-iv>

CP1, FC1 and FC5 for example, which are the closest pre-determined places for electrodes to C3. However, these places might already be too far from C3 to pick up any desirable signals.

- Lastly, every electrode is connected via a non-shielded male-to-male standard jumper cable, each of which susceptible to noise from either unwanted electromagnetic waves or vibrations of accidental movements of the test person. With double the electrodes, there was a fear of picking up an increased amount of noise which would decrease the signal quality.

The last part of the montage was to decide what kind of referencing to use. The perfect reference point would be one with zero or a constant potential, so that the measured signals from the brain correctly reflect the actions of a test person. However, such a reference point does not exist, since there will always be some sort of electrical interference on the human body.

Although not explicitly specified in the OpenBCI data-sheet, it can be assumed that the standard referencing of the headset is an unipolar "recording reference" between the ear and electrodes. This is due to the OpenBCI headset having a single earclip to be attached to the earlobe to be used as a reference point. The earlobe was most likely chosen due to its relative inactiveness in terms of brain activity and its distance to the recording electrodes (Junghöfer et al., 1999). This referencing electrode on the earlobe is used during the live-recording of data, hence the reference is called an online reference. When the reference is only decided after the recordings, it is called an offline reference. The offline reference might be useful if one would like to have more flexibility in the analysis of obtained signals. Some of the unipolar offline options are [33][23]:

- **Linked Mastoids (LM):** One of the older referencing techniques. This unipolar method assumes that average potential over two mastoids (ears) approximates zero. This method of referencing is still one of the most used referencing in neuroscience, although it has its flaws. This method is mostly used for recordings on the middle line of the scalp as there is distortion near the two ears and can be used for offline or online recordings although the latter is not recommended as physically linking the two electrodes creates a short-circuit that might disturb the distribution of voltages across the scalp.
- **Average Referencing (AR):** This unipolar method will take the average potential of all electrodes and use it as the reference signal to compare with the electrodes. This method is based on the theory that in a perfect layered spherical head with neural currents spread out in an isotropic way, the integral of all potentials over the head's surface sums up to zero [32]. The drawback of this method resides in the fact that the average human head is not spherical, homogeneous or isotropic. Next to that, the electrodes would need to be placed around the entire head's surface for AR to work perfectly, which is not feasible. Thus AR can only approximate a zero potential with sufficient (>128 channels) [33] electrodes.
- **Reference Electrode Standardization Technique (REST):** a re-referencing method using the offset voltage between an external standard reference electrode that has a stable and reproducible potential and the electrode used for referencing during the measurements. The offset voltage is determined by immersing both electrodes in an electrolyte solution and letting it reach a stable equilibrium, after which the voltage difference between the two electrodes is measured. Using this offset, a correction factor can be derived and afterwards be applied to future measurements with the calibrated reference electrode. Although this method works the best according to Yao (2019) [33], this one needs the most time-investment and is relatively complex in comparison to the previous two methods.

Another method to record data would be to use bipolar recording. Here, the voltage difference between two adjacent electrodes are constantly measured. This method of extracting data can have advantages compared to unipolar recording, the biggest one being that it can remove common artifacts that appear in both electrodes since the difference is measured between them. Still, there is a downside. If for instance a noise source comes from a certain direction in parallel with the bipolar configuration, one electrode will receive the noise a fraction sooner than the other one and the measurement will be inaccurate in the time-domain. For the OpenBCI headset that is used in this project, it was not recommended to use bipolar recording since the headset is optimized for unipolar recordings and little to no information was given on how to convert the headset to be suitable for bipolar recordings. Thus, it was decided to keep recording with a unipolar reference which is the earlobe.

As for the offline re-referencing, due to time-constraints there was no opportunity to test every method.

Only the AR re-referencing was tested, but it yielded no improvement over the standard referencing of the headset (see chapter 5); this is most probably due to the insufficient amount of channels and a lack of coverage of the head. Thus, it was chosen to do no special re-referencing and to rely on the build-in common-mode noise rejection of the bio-chip of the headset.

4.2. Software

The data acquisition software is focused on providing an optimal workspace, suitable to extract and process data of the headset efficiently. It should be able to save the acquired data into a csv-file for further analysis and it should have support for the OpenBCI "Ultracortex mark IV" and Neurosky "Mindwave MW001" headset. Besides that, one of the should requirements for the program is that it will also work with other headsets. This gives the opportunity to measure with another headset if it occurs that the OpenBCI or Neurosky headset will not work properly. The second should-requirement is that the application is able to live-stream data to other groups. This requirement is set to a should requirement but it would be nice to achieve, as this will give the opportunity to send live data to the decode group and this is a must to let the whole project work as intended. Table 4.3 shows the different software applications that were considered during the project[20].

The OpenBCI GUI is made by OpenBCI and as a consequence of this, it is fully optimized for the OpenBCI headset. A disadvantage that has a high impact, is the fact that the program has no support for other headsets, which limited the choice for a headset significantly. Although it is only compatible with the OpenBCI headset, it has a built-in impedance check for the electrodes. Additionally it gives a clear first view of all the signals.

Another program which was considered, is writing a Python code ourselves to extract and process the data. The advantage is that it is possible to integrate all components in one code. However, the main disadvantage is that there are not packages available for all headsets. Sometimes there is no manual available about which protocol the headset uses to communicate with the computer, which makes it hard to extract data without an available package.

OpenVibe [30] is a C++ based open-source software platform dedicated for designing, testing and use of brain-computer interfaces, and is specially made for real-time neuroscience. At the time of writing, OpenVIBE is supported by Inria (French Institute for Research in Computer Science and Automation). One of its most distinguishing features is its graphical language for designing signal processing chains. The disadvantage of OpenVibe is that there are limited possibilities for different methodologies as the user is limited to the built-in features of OpenVibe.

BCI2000 is, like OpenVibe, a C++ based platform. This application is not intended as a signal processing design, but it has support for a wide range of different BCI experiments. The disadvantage of BCI2000 is that only popular EEG headsets are supported by it, which does not include the Neurosky Mindwave.

Simulink is a platform for simulation and model-based design for dynamic systems, which runs under Matlab. It provides a graphical environment for processing and extracting data. Although it has no built-in support for different headsets, it is possible to use most headsets by reading out the serial port.

All considered applications can write data to a csv-file so all applications will fulfill that requirement. Another requirement that was set was that the software must have support for the OpenBCI and Neurosky Mindwave headset, which is not the case with the OpenBCI GUI and the Python code. Live streaming data to the decode group is possible with all discussed programs.

It was decided to use OpenVibe as data acquisition software. The main reason is the fact that this will work with several headsets (including the OpenBCI and Neurosky Mindwave headset), which makes it possible to switch to another headset if necessary. Besides that, OpenVibe supports live-streaming data. The OpenBCI GUI is used during the project to get a first view of the measured signals before they will be recorded with the use of OpenVibe. The reason for this is that the OpenBCI GUI gives a clear first view of the signals, with a proper y-axis and lines in the graph. OpenVibe does not provide such functions.

Software	Advantages	Disadvantages
OpenBCI GUI	<ul style="list-style-type: none"> • Optimized for OpenBCI headset • IP/TCP streaming to external program • In-built impedance check • Good first view of signals 	<ul style="list-style-type: none"> • No support for other headsets • No possibility to integrate all components • Extra code/application needed to process all data
Python	<ul style="list-style-type: none"> • Built-in integration of all components • Package available for OpenBCI 	<ul style="list-style-type: none"> • Not for all headsets packages available (including the Neurosky Mindwave) • No graphical interface
OpenVibe	<ul style="list-style-type: none"> • Support for different headsets • Specially made for BCI • Possibility to integrate all components • IP/TCP streaming to external program • Possible to do in-built processing using Matlab or Python • Graphical interface 	<ul style="list-style-type: none"> • Limited scenarios possible • No proper first view of signals
BCI2000	<ul style="list-style-type: none"> • Real-time processing • Specially made for BCI • Support for different hardware • Limited graphical interface 	<ul style="list-style-type: none"> • Not intended as signal processing design • No in-built TCP streaming • Limited support in previous years. • No support for the Neurosky Mindwave
Simulink	<ul style="list-style-type: none"> • IP/TCP receiving and streaming to external program • Runs in Matlab environment • Specially made for live signal processing 	<ul style="list-style-type: none"> • No in-built support for different headsets

Table 4.3: Comparison of different acquisition applications [20]

OpenVibe

As described earlier, it was decided to use OpenVibe during this project. OpenVibe consists of two main components: the acquisition server and the designer [30].

The acquisition server provides the connection between the incoming signals from the headset and the designer. It will read out the connected USB port and will access the device using the protocol from the manufacturer. The acquisition server supports different kind of headsets, like EEG or MEG systems, and different brands and models, but it has to be mentioned that not all supported headsets are stable. This will be indicated in the acquisition server setup with 'unstable' behind the specific headset. In section 3.2, several different headsets were discussed. The acquisition server has built-in support for the OpenBCI and Neurosky Mindwave headset. OpenVibe has no in-built support for the Emotiv EPOC and the InterAxon Muse 2, but this can be fixed by using the LabStreamingLayer (LSL) which will need additional acquisition software that delivers the acquired data to the acquisition server. This property allows the user to create a hardware independent scenario. The acquisition box sends the information to the acquisition client box in the designer using an IP port, which can be specified in the acquisition server. The acquisition server will then send the data to the designer per block; the amount of samples

can be adjusted under 'Sample count per sent block'. The default value is 32 samples per block. The receiving applications can later convert the data to new buffer sizes (the buffers are usually called epochs if they have been segmented from the signal stream using specific rules).

The designer is the main component of OpenVibe. The designer gives a visual interface for designing scenarios. This can be done using the available boxes in the environment. These boxes can be connected by lines to forward the data between boxes. There are several boxes available, but the most important ones are: acquisition client, temporal filter and csv file writer. The acquisition client reads out the data (in microvolt) from the acquisition server using the same IP port as the acquisition server. The temporal filter box will filter the data using the specified configuration. There are two filter methods available, Butterworth and Chebyshev. Additionally the specifications of the used filter can be specified, like the filter type, order, pass band ripple and cut frequencies. The csv file writer writes the incoming data to a csv file, with a default precision of 10 decimals. Figure B.3 shows a scenario which is regularly used during the project. This scenario will run a video and will store the data in a csv file. This scenario contains of an acquisition client, two filters and a csv file writer (which were all discussed before). Besides that, it contains of the Graz motor imagery BCI stimulator box. This box will run a program programmed (in lua programming language) by the user and will visualize it using the Graz visualisation. The Graz motor imagery BCI stimulator box will send a signal to the csv writer if a stimulation is sent, which will add an extra column to the csv file for the eventstamp, which marks the exact time a stimulation occurred.

OpenVibe supports different kinds of live streaming. This can be done built-in by using the Python or Matlab box. This allows the user to integrate everything in one program and to use the visual interface of OpenVibe. During the project it was found that integration using this method is very difficult, due to the specific Python layout required by OpenVibe. Instead of integrating all components inside the OpenVibe program, it can also be done by sending data on an IP port to an external program. This data stream can be read by other groups if they want. This way of integrating all components has not yet been tested in the project.

OpenBCI GUI

As stated earlier, OpenVibe gives no proper fast view of the quality of the measured signals. As a consequence of this, the OpenBCI GUI is used to check the signals of each electrode before recording it with OpenVibe. This will decrease the chance of a bad recording, where one of the electrodes is not working. The OpenBCI GUI will display the railing of each electrode, railing indicates that the measured value is beyond the displayable range of $-10000\mu V$ to $10000\mu V$, meaning the data is clipping. This is displayed in a range of 0 % to 100 % in which 100% means clipping. Figure B.5 shows an example of how the OpenBCI GUI shows the railing per channel.

Additionally, a visual check is done. A visual check can be done by checking the presence of a blinking spike on electrode Fp1 and Fp2, because blinking will give a peak with an amplitude which is higher compared to the brain activity on both electrodes [2]. The last check that can be done is to check for alpha waves. The frequency of an alpha wave ranges from 7 to 12 Hz and can be found in the posterior regions of the head on either side. The locations P3 and P4 will best meet this location. A higher amplitude will be found on the dominant side of the subject. Alpha waves are salient during relaxed wakefulness with eyes closed (resting visual cortex), which also occurs during REM sleep [24]. Figure B.5 shows an example of an alpha wave using the OpenBCI GUI on channel 7 and 8. The alpha wave can be detected using the characteristics described before. It can be found that there is an alpha wave between approximately -3.5 seconds and -2.5 seconds. Which is repeated at around -2 seconds to -1 second.

4.3. Pre-processing

The measurements will probably not only contain pure brain activity, but also activity from muscles and other physical artifacts. As these signals are unwanted, there is the need to filter out these artifacts as much as possible. The different frequencies can be divided in different bands: Delta(0.5-3Hz) , Theta(3-7Hz) , Alpha(7-12), Beta(12-35) and Gamma (35Hz>) [3]. The Delta band will mostly occur during sleep, the Theta will be occur if a subject is deeply relaxed or inward focused. The Alpha band will be recognizable when the subject is very relaxed and with passive attention. The beta band will say something about the anxiety dominance, active, external attentions and how relaxed someone is. The highest frequency band (gamma) will say something about the concentration of the subject [1]. The

frequency of the muscles are around 30 to 80 Hz. As a consequence, the gamma band, which are all frequencies above 35 Hz, is the most vulnerable to muscle artifacts [5]. To filter this, first a bandpass filter from 0.5-30 Hz (fourth order butterworth) was used. The working of this filter will be shortly analysed in section 5.2. Figure B.4 shows the frequency response of this filter.

The frequencies that are correlated to movement-related processing such as motor imagery and execution are in the range from around 7 to 30 Hz [14][15]. As a consequence, a new bandpass filter is designed which is a fourth order Butterworth filter from 7 to 30 Hz. The working of this filter will be analysed in section 5.2. Figure B.4 shows the frequency response of this filter.

Additionally, there is a notch filter around 50 Hz. This filter is implemented using a bandstop (fourth order Butterworth) filter from 48-52 Hz. This filter is needed to filter out the frequencies from the power supply, as this will give interference when the laptop is connected to the power supply. Figure B.4 shows the frequency response of the used filters.

4.4. Paradigms

For this project, we want to see if it is possible to distinguish motor control/motor imagery. For this, different measuring methods are used as probably not all methods will give the best result. The results of the used methods will be discussed in chapter 5. The different methods will be discussed in this section:

- Method A: The goal of this experiment was to distinguish between left and right motor control. The first 20 seconds of the experiment were used to let the subject relax and are needed for the headset to stabilize. After this rest period, the subject was asked to clench one of their hands three times. This sign is given every 10 seconds by someone who is next to the subject. There are two different sequences made to ensure the subject doesn't know which command is coming. Every measurement consists of 12 trials (right or left hand clench).
- Method B: The goal of this experiment is to distinguish between rest and a motor control task. This experiment is 60 seconds long with a stimulation at 30 seconds. The subject was asked to clench both hands once. There was no extra rest period in this experiment.
- Method C: This experiment is somewhat different compared to the previous two, as the subject was asked to clench their hands for 30 seconds. This implies that the subject has to clench their both hands, open them and clench them again until the 30 seconds are over. There is a 10 seconds rest period before and after the activity. The start and stop stimulation are given manually by someone who is next to the subject.
- Method D: This experiment was established after it was possible to make a video with OpenVibe. This experiment follows the same methodology as method A, but can run without an extra person. A video is setup to ensure the consistency of the measurement. Each measurement contains 10 trials (5 right and 5 left), with a 10 second rest period before the trials. At the beginning of a trial, a cross will be shown on the screen. After 2 seconds, there will be an alert beep to attend the subject that a stimulation is coming. One second later, a left or right arrow is shown on the screen, which will stay 2 seconds. The subject is asked to clench their right or left hand (which is randomly determined by the video) once the arrow appears. After that, a final 5 seconds black screen will be shown as rest period. After that, a new trial will start. Every trial will follow the same procedure. This method is used to acquire training data for training the model of the decode group. The OpenVibe scenario that is based on this methodology can be found in Figure B.3.
- Method E: This method is based on method C, but it will be more consistent. This is done by using a short video instead of a extra person next to the subject. The experiment begins with a 10 second long rest period. After 10 seconds, there is an alert beep. The subject is asked to clench both hands when they heard the alert beep. The experiment will stop after 15 seconds.

Figure B.2 shows an overview of the different methods that were used during the project.

5

Data analysis

In this chapter, the data extracted from the OpenBCI Ultracortex "Mark IV" EEG Headset will be plotted and analysed. First, the methods to transform the data received in time-domain to frequency-domain will be explained. Secondly, the results from the measurements are plotted and analysed, after which methods and results to potentially improve the signal are shown. Lastly, the importance of consistency of the experiments and the focus of test subjects are discussed.

5.1. Background

First and foremost, one of the most important mathematical technique used in the analysis of EEG will be briefly explained: The Fourier transform. Using this transform, it is possible to discover which frequencies are most dominant in a signal. The continuous Fourier transform is given by the mathematical formula:

$$F(\omega) = \int_{-\infty}^{\infty} f(t)e^{-i\omega t} dt \quad (5.1)$$

Where $F(\omega)$ is the transformed function in frequency domain, $f(t)$ is the original signal in time-domain, ω is the angular frequency and t is the time variable, integrated over all time values.

Its discrete version, also called DFT, is given by:

$$X[k] = \sum_{n=0}^{N-1} x[n]e^{-\frac{j2\pi kn}{N}} \quad (5.2)$$

Where $X[k]$ represents the complex amplitude of the k -th frequency component. $x[n]$ is the discrete-time original signal of length N . Which is multiplied with a complex exponential and summed for all values from $n=0$ till $N-1$.

In the analysis of the recorded data, two variations of the Discrete Fourier transform (DFT) are used: the Fast Fourier Transform (FFT) and the Short-Time Fourier Transform (STFT).

- The FFT algorithm is used to obtain the power spectral density (PSD) plot of a segment of the recorded signal by squaring the absolute value of the FFT and dividing by the total amount of samples. Although the "original" Discrete Fourier transform could be used, the FFT algorithm is able to compute the power of the frequencies at a time complexity of $O(N \log(N))$, whereas the DFT has a time complexity of $O(N^2)$. Due to the FFT's speed, it is more suitable for transforming the signal in real-time if needed. By splitting the input data sequence into halves until it reaches a base case of a subsequence with length 2 (divide-and-conquer). Then by multiplying the elements in a single subsequence with a precomputed factor and combining the different subsequences into bigger sequences, until the original length is achieved and rearranging the sequence, the PSD is calculated given in units of μV^2 . Not $\mu V^2/Hz$ due to it being the discrete transform and the signal is not integrated over time but dimensionless samples. As in the case of the continuous Fourier transform.
- The STFT variation of the Fourier transform was used to obtain the spectrogram of a recorded signal. The spectrogram is a two-dimensional plot that shows the magnitude of a frequency at

a certain moment in time, which is useful to look for activity at a specific timestamp. Like the FFT, the STFT takes input discrete signals as input as well as produces them. Difference is that instead of transforming the whole signal into the frequency-domain like the FFT does, it applies the Fourier transform to overlapping time windows. The most simple window is a rectangular window. However, this window is not optimal to calculate the STFT of EEG signals due to its high main lobe, meaning that adjacent frequencies do not get attenuated and can interfere with each other causing spectral leakage. Fortunately, there are many other windows to choose from with better attenuation of adjacent frequencies such as a Hamming, Hann, Kaiser and Blackman window. In our application, it was chosen to use a Hann window due to its widespread use for random signals [17] and its all-around capability to produce a, not optimal, but fair frequency resolution and good spectral leakage protection compared to the other windows [9]. Depending on the signal frequency, the window size and the amount of overlap between the windows, a certain time or frequency resolution of the STFT analysis can be reached. By having a lot of overlap and thus more redundancy, the time resolution increases, but the frequency resolution decreases due to a reduced amount of independent segments the STFT can analyse. With little overlap, the inverse happens of the latter. Same for the window size, a bigger window size results in a decrease in time resolution, but a increase in frequency resolution, whereas a smaller window results in exactly the inverse.

Lastly, the magnitude of each block in the spectrogram is given in μV since this spectrogram is the summation of magnitude, and not power, of the frequencies.

5.2. Pre-processing

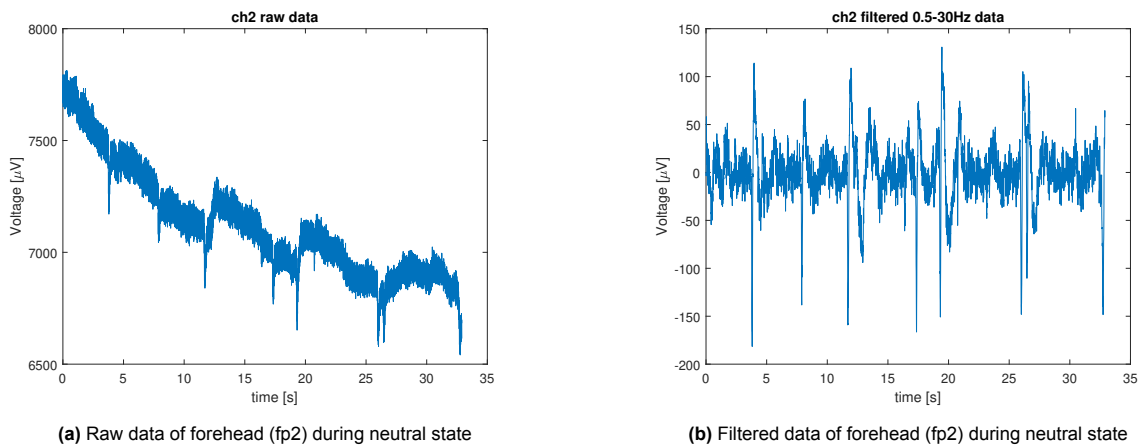


Figure 5.1: Raw (Figure 5.1a) and filtered data (Figure 5.1b) of position Fp2 during neutral state; drift and high frequency noise occurring in the raw data is filtered out by a 0.5 - 30 Hz bandpass filter; which can also be used to show eye blinks.

First we tried to measure someone's neutral state with occasionally some blinking. If looked at the electrode at the forehead, which is channel 2 at position Fp2, although some peaks can be seen that represent blinking, the raw data cannot be used for processing due to the amount of high frequencies in the signal and the DC component pushing the measurement to $7500\mu V$ as seen in Figure 5.1a. It was found that the frequency that correlates with motor imagery is from around 7 to 30 Hz [14]. However, looking at dataset III used for motor imagery experiments from a BCI competition held in 2002 [4], a bandpass filter of 0.5 to 30 Hz was used, so it was decided to try that filter first and see whether it would work. Which produced Figure 5.1b when tested with the same data. This centered the signal around zero volts and reduced the amount high frequencies drastically and the moment of eye-blinks could easier be detected. Although this filter seemed to work at first, when we plotted the STFT spectrogram (see Figure 5.2a) of the data, most of the power is still around the DC component, which is not unexpected. By looking at the unfiltered FFT plot (Figure C.1), it can be seen that the DC component is magnitudes higher than the rest of the frequencies, meaning that a filter with a lower bound of 0.5 Hz was not able to cancel out the DC components. Together with the decoding subgroup, it was decided that a 7 till 30 Hz, fourth-order bandpass butter-worth filter served the best filtering properties in order

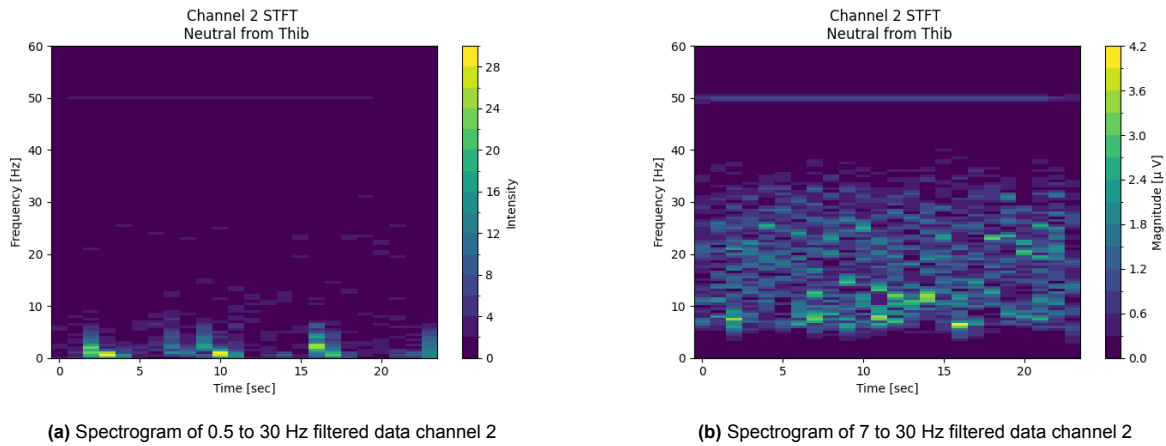


Figure 5.2: Spectrograms of signals using different filters 0.5 - 30 Hz (Figure 5.2a) versus 7 - 30 Hz (Figure 5.2b). By taking 0.5 Hz as lower bound, it does not reduce DC component enough. Raising the lower bound to 7 Hz solves that problem

to filter the raw data such that the DC components are removed, but saving enough bandwidth for the decoding team to get enough data for their test and training data. Applying the improved filter yields the result in Figure 5.2b. It shows that the magnitude of the signal around the DC component has been reduced, such that the other frequencies are better visible on the spectrogram. Notice that there is a faint line at 50Hz, this is due to the many power outlets radiating a 50Hz frequency in close proximity to the headset, increasing the noise that the headset receives. This problem was fixed by applying a notch filter from 48 - 52 Hz and record data further from power outlets.

5.3. Measurements

To see how well the headset could pick-up instructions from merely brain signals, the experiment complexity was increased step-by-step. As shown in the previous section, the neutral state was first measured mostly to verify whether the headset could receive an arbitrary signal and to test the functionality of the filters. The next step was to verify whether the received brain signals generated by blinking were distinct enough for the decoding subgroup to train a model, in order to filter them out from the recording.

5.3.1. Blinking

In the blinking experiment, the subject was asked to blink every three seconds when audio cue is given, 10 seconds after the recording is started. If the headset would work correctly, one would expect to see activity at the front-side of the head at the exact moment the subject blinks. By measuring the electrode on the forehead (Fp2), the time plots are obtained can be found in Figure 5.3a, Figure 5.3b and Figure 5.3c.

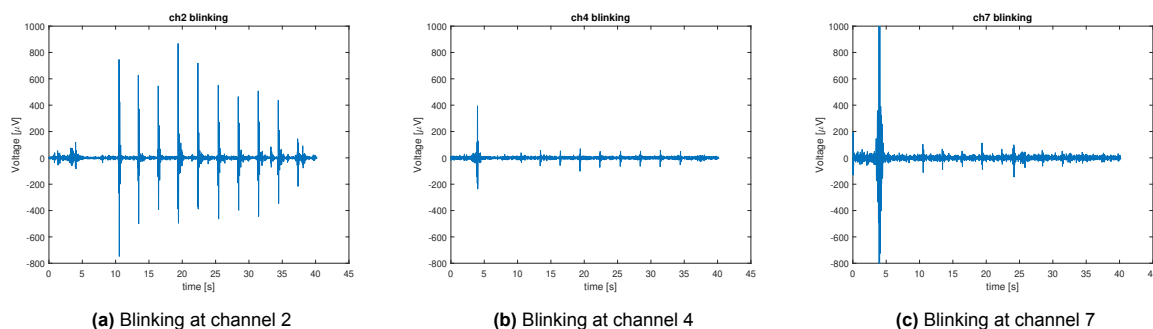


Figure 5.3: Blinking magnitude in time-domain at channel 2 (Figure 5.3a), 4 (Figure 5.3b) and 7 (Figure 5.3c). It can be seen that the further away from the forehead, the weaker the blinking signal gets. To detect eye blinks, measure on channels 1 and 2. Also recommended to always cut away the first 10 seconds of recorded data to cut away anomalies.

It can be clearly observed that each time when the subject was blinking, a distinct voltage peak was generated at the Fp2 position (channel 2). Looking at the other channels at the center of the head (channel 4) and the back of the head (channel 7), the blinking signal gets progressively harder to distinguish from the noise. This indicates that the headset can in fact detect signals correctly at the right places on the brain.

Another thing to notice is that during the first five seconds of the recording, anomalies occur in the signal. Looking at the time plots, sudden peaks at the beginning of the recordings can be seen. Consequently, the first 10 seconds of all the following recordings were always cut off before analysing the measurements.

5.3.2. Motor execution

Following blinking, the next step was to detect brain signals on the top of the head by moving the left and right hand. In general, what is to be expected is that at the time of a movement of either hands, an change in power at the alpha band (7 - 12 Hz) and beta band (12 - 30 Hz) is observed [29]. Next to that, the helmet should be able to detect the change in magnitude close to the exact time that a subject moves its hands [28]. Lastly it is expected that the movement of the left hand will induce a bigger power change than the right hand in the right hemisphere of the brain and vice versa [27].

Thus, the first thing to test was to confirm that the headset is able to detect the movement of either hands. This was done by making a recording of fifteen seconds long and letting the subject clench both their hands a single time when a audio cue was given at $t = 10s$, which corresponds to method E described in section 4.4. Afterwards, the subject was instructed to stay still and do nothing except involuntarily blinking. Using the recorded data, power spectrum density (PSD) plots were generated such as the plot of channel 6 (Figure 5.4a), plotting a one second fragment of the exact time when a subject moves its hands versus a one second fragment where the subject was not doing anything.

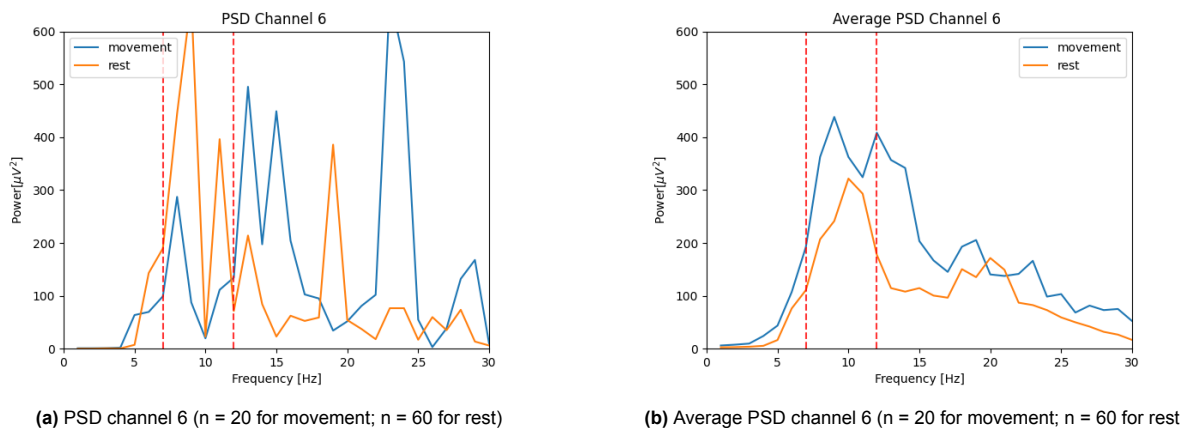


Figure 5.4: PSD of a single recording of 1 second (Figure 5.4a) and of an average of 20 recordings of movement and 60 recordings of rest, both of which are 1 second (Figure 5.4b) at channel 6 comparing movement vs rest. With a single recording, no coherent conclusion can be deduced. However with an average of recordings, it can be clearly seen that there is a change in power during movement compared to during rest. Thus the headset is able to differentiate two classes

With the plots, no coherent conclusion can be deduced due to the inconsistency of the signal across all the different channels. The solution to this inconsistency is the averaging of data between all the trials of this experiment. In Figure 5.4b the PSD during movement is an average composed of one second fragments across 20 trials and the PSD during rest is an average composed of 60 segments of one second across 3 measurements. Looking at the averaged plot, it can be seen that the data is much more consistent across all frequencies and that the power during movement is higher than the power during rest in the alpha and beta band. However by looking at the plots in Figure C.3 of all relevant channels for motor execution, it can be seen that channel 4 at position Cz on the head is the only one not showing any major differences between movement and rest, which indicates that Cz might not be optimal for detecting motor execution signals.

Although the PSD plots hinted that the headset is able to distinguish between movement and rest, the PSD works best with stationary signals while brain signals are non-stationary. To see the performance of the headset as a function of time, the STFT is used to generate a spectrogram. For the experiment, a subject is tasked to clench either their left or right hand for each trial instructed by a video, as described by method D described in section 4.4. To see if the headset is able to detect the brain signals to move either hand, the data from trials for left and right hands are taken as one conjoined data set.

Like the PSD plot, generating a spectrogram plot from only one measurement will yield unreliable results even if it might look like it corresponds with a hypothesis. For the following spectrograms in this report, a Hann window with an overlap of 80% is used and a width of 0.5 seconds. With a sampling frequency of 250 Hz of the headset, the time-resolution becomes 100ms. Of course, other window sizes can be used. For example a smaller window size of 0.1 second (see Figure C.4) to increase time-resolution, but then it can be seen in the spectrograms that the frequency resolution is very low like explained in section 5.1, with the magnitudes of 5 - 15 Hz being lumped together. The inverse happens with a time window of 1 second (see Figure C.5), where the frequency-resolution has clearly improved, but the exact time of peaks is hard to pinpoint. So a compromise of a 0.5s window seemed logical.

Looking at plot Figure 5.5a which is zoomed in at a four second fragment of a trial where a visual cue was given at $t = 2s$, there is a peak that begins around $t = 2.5s$, 0.5 seconds after the visual cue was given, which corresponds with the average reaction time of 250 ms of a human[12]. Still, by averaging over multiple trials, more certainty can be given about the correct functioning of the headset. In the case of plot Figure 5.5b, an average over 60 trials ($n = 60$) was taken. The data of these trials are also sent to the decode group and used to train their decoding model.

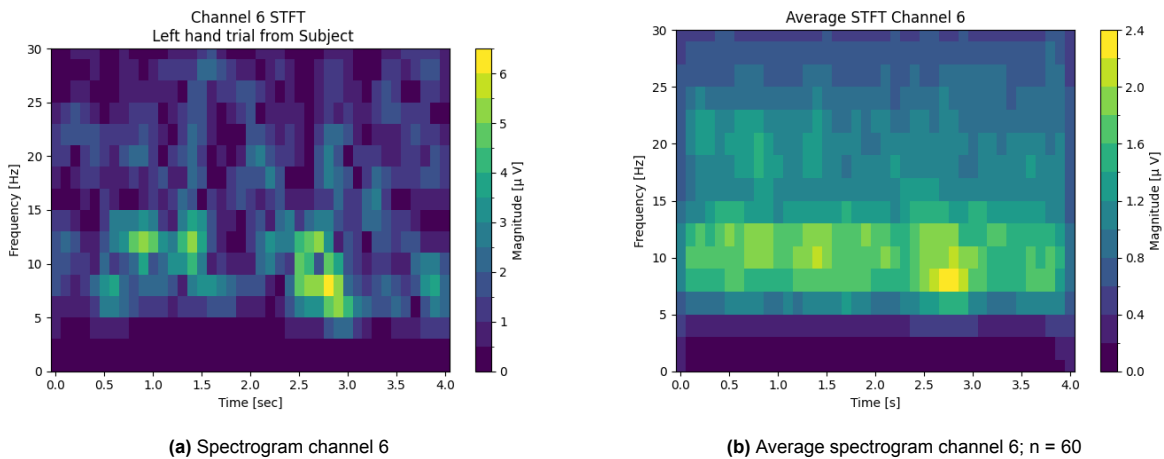


Figure 5.5: Spectrogram of a single recording (Figure 5.5a) versus one of an average of 60 recordings (Figure 5.5b). Both show a peak around 2.5 seconds, but the average spectrogram on the right confirms that the change in magnitude is consistent around 2.5 seconds. Since the visual cue is at 2 seconds and the average human reaction is 250 ms [12], the timing of the peak correlates with the visual cue

Although the spectrogram showed there is a change in magnitude after the visual cue, it is hard to draw a conclusion from it since the spectrogram looks rather monochrome and only peaks are made a bright colour, while dips compared to the average signal before the cue stay dark blue. To better represent the changes in the alpha band, the magnitudes of the alpha band in Figure 5.5b are summed, averaged and plotted on a magnitude-time scale with a standard error of $\frac{\sigma}{\sqrt{n}}$, with σ the standard deviation and n the amount of trials, the magnitude plots in Figure 5.6 are obtained. With this, it can more clearly be seen that there is a change in magnitude around the time of the visual cue at $t = 2s$ (red dotted line). When the magnitude becomes lower than the average magnitude before the visual cue, it is called event-related desynchronization(ERD). On the other hand, if it becomes higher, it is called event-related synchronization(ERS). According to studies[28], (imagery) hand movements mostly result in ERD at the moment of a cue and afterwards stabilises again to pre-cue level. Looking at channel 4 (Figure 5.6a) located the center of the head and channel 5 (Figure 5.6b) located on the left side of the head, the difference between rest and movement can even be seen due to a noticeable dip (ERD) in magnitude at the time of the visual cue. However, it sometimes it can happen that after a ERD, a ERS occurs [27]. Channel 6 (Figure 5.6c) located on the right side of the head, exhibits such an ERS after a ERD. For

all channels, a factor of around 1.5 in difference between the extremes after the cue and the average before the cue can be seen. However, one would expect the dip to occur right after the time of the visual cue, but in the plots it happens around 0.5s beforehand. This might be due to the window size, which is also 0.5s, already calculating the STFT for the timestamps before the cue with data after the cue, hence the dip before the red dotted line.

Notice the sudden drop in voltage at the zero and four second mark, that is not the headset losing power, but the Hann window tapering the edges of the data towards zero.

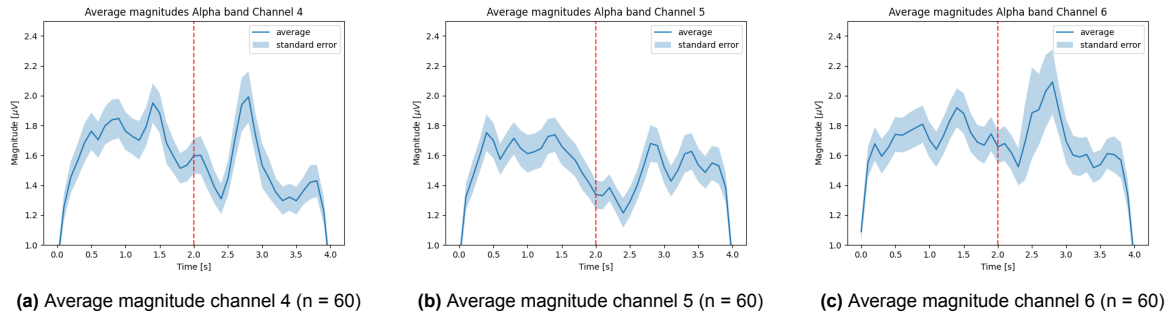


Figure 5.6: Average magnitude across 60 trials of channel 4 at Cz (Figure 5.6a), 5 at C3 (Figure 5.6b) and channel 6 at C4 (Figure 5.6c). For channels 4 and 5, an ERD (decreased magnitude than average before the cue) can be seen around the time of the visual cue at $t = 2s$. For channel 6, a ERD can also be seen at $t = 2s$, but afterwards also a ERS (increased magnitude). It can be concluded that the headset is able to differ movement from a neutral state at the time of the visual cue.

Looking at channel 7 and 8 (Figure C.6e and Figure C.6f) it is seen that those two channels do not produce a distinct ERS and ERD with reference to the signal before the cue. This could indicate that channels 7 and 8 might be too far from the active regions during motor execution. Next to that, it was seen that the average magnitudes of the beta band (12-30 Hz) looked flat throughout the trial as shown in Figure C.8 in the appendix, except for channel 3 where a slight ERD followed by a ERS was seen after the cue. Nevertheless, compared to the alpha band, the magnitude difference between before and after the cue is minimal in the beta band. As a consequence, it was decided to not use the beta band to draw conclusions.

Lastly, to investigate whether a difference between left and right can be seen in the data. The average sum of voltages in the alpha band is again taken. However, this time the trials are split into 30 left hand trials (movement of left hand) and 30 right hand trials (movement of right hand). Since right hand movement activates the left hemisphere and vice versa, it is expected that channel 5 exhibits increased ERD and ERS during right hand trials and channel 6 the same during left hand trials[28]. Whereas the channels in the center of the head do not have a large difference in synchronization activities since they should receive equal amount of stimulation from both the left and right hemisphere of the brain. Following the same method and using the same dataset as the previous paragraph, the plots for channel 5 and 6 were produced, which can be found in Figure 5.7.

It can be seen that for channel 5 (left hemisphere), the right trials produce a stronger ERD response compared to the left hand trials in reference to the pre-cue magnitude of around $1.6\mu V$ (green dotted line), which indicates that the right hand causes more activity on the left hemisphere of the brain. Looking at channel 6 (right hemisphere), the inverse can be said. Here, it is seen that the left hand trials show more ERD and ERS than the right hand trials, indicating that the left hand plays a larger role in the right hemisphere of the brain. A smaller detail that can be seen is that while the "stronger" hand begins with ERD at the visual cue, around 0.2 seconds later, the "weaker" hand initiates ERS, meaning that while one side of the brain invokes more potential, the other side of the brain does the inverse for a brief moment.

The results for channel 3 and 4 can be found in Figure 5.8. Looking at both channels, albeit not exactly the same magnitude between the left and right hand trial. The shape of both trials per channel still look like they fluctuate up and down at the same time, meaning both left and right hands have an even impact on their respective area at the scalp.

Looking at the beta band plots in the appendix Figure C.9, it is seen that except for channel 3 and 5, the difference of before and after the cue is not convincing, further confirming they should not be used

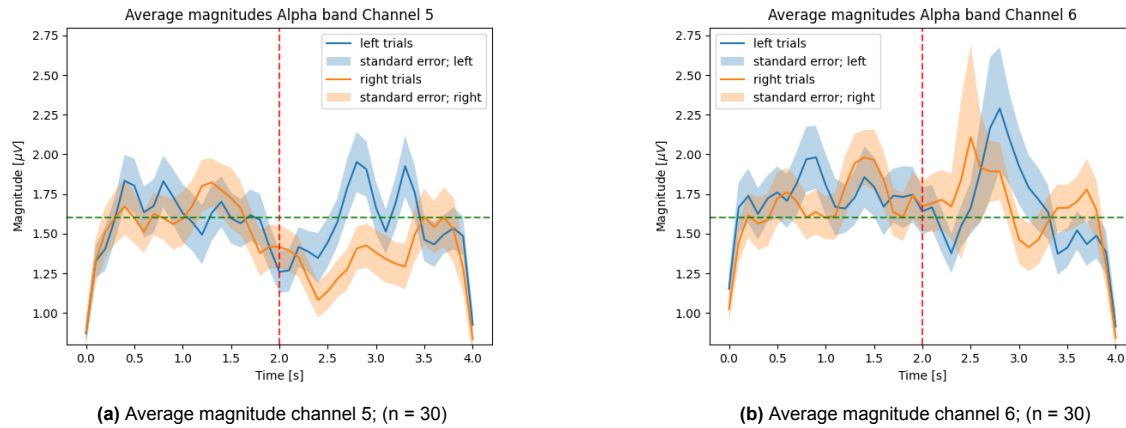


Figure 5.7: Magnitude plots of left and right trial at channel 5; left hemisphere of the brain(Figure 5.7a) and channel 6; right hemisphere of the brain(Figure 5.7b). At channel 5 the right hand produces a stronger ERD than the left hand and at channel 6 the left hand produces a slightly stronger ERD and ERS then the right hand. This corresponds to the fact that the left hand movement invokes a stronger response in the right hemisphere of the brain at C4 and the right hand a stronger response in the left hemisphere at C3 [28] and the headset might be able to differ left hand movement from right hand movement. However, the difference between left trials and right trials is too small to give a solid conclusion.

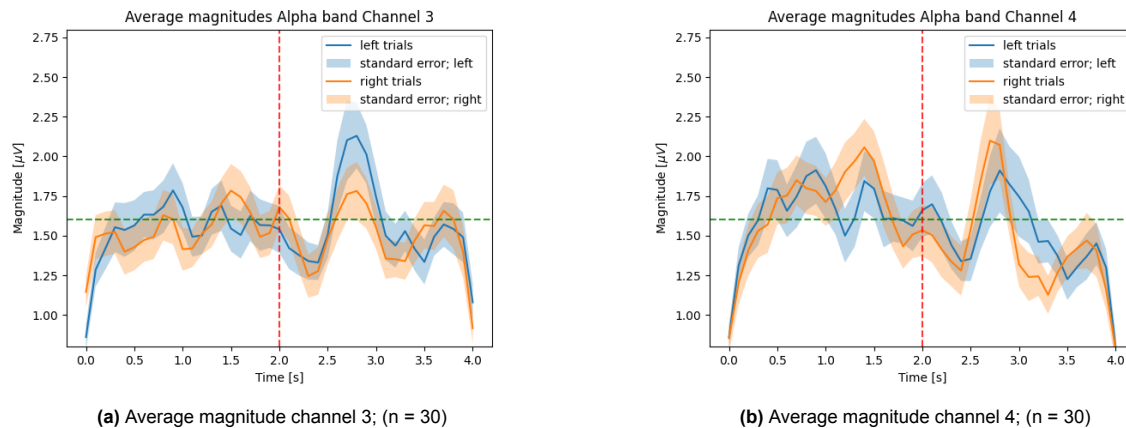


Figure 5.8: Magnitude plots of left and right trial at channel 3 Figure 5.8a at Fz and Figure 5.8b at Cz, both located at the center line of the scalp. It can be seen that both left and right hand trials fluctuate the same way for both channels, meaning both channels receive an even impact from the left and right hemisphere of the brain.

to draw conclusions.

All in all, it seems that the headset is able to differentiate between left and right hand movements in the alpha band. Nevertheless, only taking the changes in magnitude as the sole feature to differentiate the movement of either hands is not recommended, since the effect of ERD and ERS might differ per subject and the results of both trials are too close to each other to give a solid conclusion.

5.3.3. Motor imagery

The last step was to test whether it could be detected when a subject is only thinking of moving its hands. Motor imagery was chosen as the hardest of all computer control signals since it is a weak signal from the brain and thus hard to determine whether a change in the EEG-signal is actually due to the motor imagery or another impulse from the brain. To generate 'valid' motor imagery signals, it requires the subject to have immense focus [26]. This focus is dependent on many factors under which the mental state of the subject and even their posture in which they sit. A upright sitting position proved to be beneficial for an increase in attention of the subject [26].

It was expected that experiments with motor imagery would yield the same results as the ones with motor execution, albeit with perhaps less distinct peaks in the magnitude plots of the alpha wave. Un-

fortunately, due to time restraints it was not possible to test motor imagery.

5.4. Quality improvement

To increase the visibility of event related potentials in the EEG signals it is needed to decrease the noise as much as possible.

5.4.1. Human antenna

Firstly, it should be explained where noise may come from. As stated before in section 5.2, the 50 Hz interference comes from power outlets. This is because individuals can couple capacitively with electromagnetic waves present in the area, functioning like an antenna of some sort.

Figure C.10a shows the voltage over time and the frequency (Bottom of figure) of the emitted signal of an individual having the probe softly in the thumb of its right hand. Its left hand in this experiment is close (approx. 1 m) to an active power supply. It can be seen that the 50Hz interference from the power supply is strongly visible. Even more interference is detected if a laptop charger is close (approx. 1 m) to the subject (Figure C.10b), it can be seen that there is still a strong 50 Hz component in the signal, but now mixed with other frequencies. The effect of a power outlet can be seen in a spectrogram like Figure 5.2b, where a noticeable 50 Hz line is seen. Figure C.10c shows the voltage when the subject still has the probe in his right hand, but is at a distance of around two metres from the power supply. As can be seen, there is significantly less interference from the power supply. So to reduce this interference, a subject should be put farther away from power outlets and a notch filter can be used to filter out the 50 Hz.

5.4.2. Pre-cautions

Some simple measures were taken to potentially decrease the noise in recordings.

- As seen in the the previous subsection 5.4.1, the further the subject is from a power outlet, the weaker the coupling and thus the antenna effect of the human body. Thus, it was decided to place a subject at least two metres from a power outlet.
- Since humans can act as antennas for EM waves, it is best to not let another person near the subject during a recording session, since the electrodes might pickup unwanted frequencies. Because of this, it was decided that nobody can come inside a radius of two metres of the subject during recording.
- It was seen that if the laptop, on which the Bluetooth dongle of the openBCI headset was connected, was charging during a recording. Distortions would be produced in the measured signal and be amplified if a person were to also touch the laptop during recording. Due to this, unplug the charger from the laptop and the power outlet.

5.4.3. Noise reduction

In the previous section all pre-cautions were discussed. More methods will be discussed in the following paragraphs to potentially reduce the noise.

Grounding

It was thought that grounding a subject might reduce the amount of noise the headset receives. This is because when a subject is grounded, the electromagnetic interference in a building on the subject drastically reduces as seen in Figure C.11a, due to the ground providing a low impedance path for the interference to flow away. Next to that, it was also experimented with aluminium foil to see if it could provide some sort of shielding against the interference for the non-shielded jumper cables. Wrapping the charger in aluminium foil and grounding the foil yielded the result seen in Figure C.11b. It can be seen that the interference of the charger has been reduced drastically or even cancelled and only the interference from other power outlets remain.

Although initially it was thought to wrap the headset in aluminium foil and to ground the subject during a recording session. It was chosen not to do so, because it was found that the internal amplifier of the headset already has an extra measure to reduce noise. The right ear clip of the headset is used for common mode noise rejection, which should already cancel out most of the noise across all electrodes.

Inside versus outside

To determine whether the electromagnetic waves generated by power outlets and cables within a building are actually distorting the measurements. A baseline of noise should be determined. To do that, a watermelon is used. A watermelon was used because of the fact that a watermelon consists of more than 95% water, making it a good candidate to imitate a human head. In addition, a watermelon emits no internal signals, so all the measured signals must be either from internal noise of the headset or coming from an external source. Consequently, our hypothesis was that if the headset had a bad common-mode rejection ratio and if the headset had a bad reference and hence not differentiating the signal well between scalp and earlobe, a higher noise level would be measured inside a building compared to the outside.

Of course, this hypothesis can only be proven if the watermelon actually is able to couple with the EM waves present and function as an antenna like the human body. To prove that is able to, the watermelon was brought inside and measured with the oscilloscope just like it was done with a human.

As can be seen in C.12, it gives the same response as the human head, albeit with a lower amplitude. Now it is known that a melon can in fact couple with EM waves, the headset can be put on on the watermelon to see whether the signal inside is any different from outside.

Figure C.13b shows the voltage plot of the watermelon outside from the tenth second of recording. It can be seen that the magnitude of the measured signal is around $2 * 10^{-9} \mu V$, which is also the baseline of the noise the headset can receive. Figure C.13a shows the voltage plot of the watermelon in time-domain, again with the first ten seconds omitted, measured inside a building. It shows that the measured magnitude is also around $2 * 10^{-9} \mu V$. From this it can be concluded that there is no extra external noise added inside a building and that the recording reference and the common mode noise rejection of the headset work as intended. To further confirm our hypothesis, a measurement of voluntary blinking was also made inside and outside. Again, it can be seen in Figure C.14 that the magnitudes of the peaks from eye blinks are almost equal for both inside and outside measurements. further solidifying our argument that the CMR of OpenBCI headset works as intended.

Re-referencing

As discussed in section 4.1, only (common) average referencing (CAR) was tested as a re-referencing method to potentially increase the signal quality. However the results plotted in Figure 5.9 show that the re-referencing does not improve the signal we had obtained without the CAR method. Due to this, it was chosen not to use common average referencing to improve the obtained measurement.

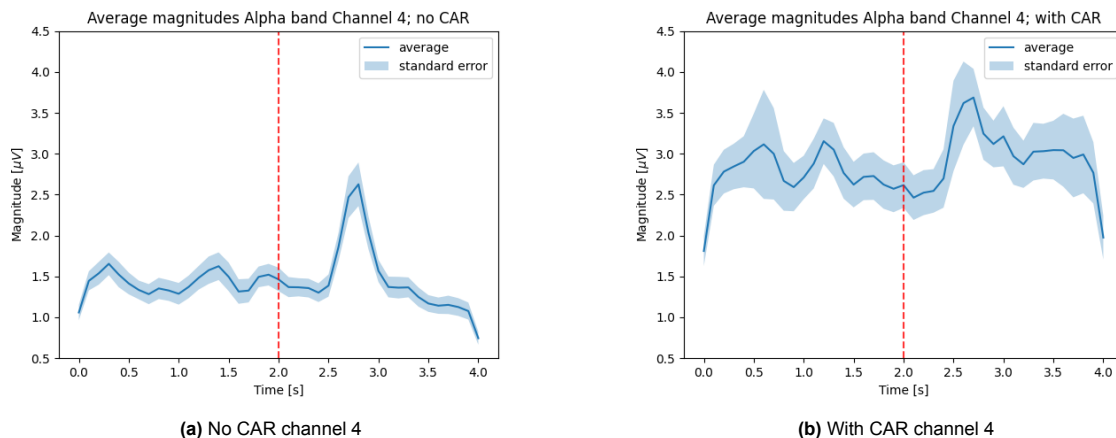


Figure 5.9: Difference in magnitude between measurement without CAR (Figure 5.9a) and with CAR. With CAR, it can be seen that standard deviation grows and the signal gets flatter overall. Measurements without CAR look more coherent with bigger differences between after the cue and before the cue.

5.5. Consistency

Although the produced plots in section 5.3 can be used to conclude the headset can detect motor execution signals. Consistently obtaining coherent data proved to be a hard task and could be due to multiple factors. One of them is a phenomenon called "BCI illiteracy". According to some studies[18][31], there is a possibility that some brains of subjects might not respond, or just a little, to an event of a paradigm. Despite the fact that the percentage of BCI illiteracy is much higher with motor imagery paradigms (53.7% over 54 subjects[31]), event related potential paradigms(11.1% over 54 subjects[31]) such like ours could still have been affected by a subject being BCI illiterate. That might be the reason some of our own recorded data not seem to contain distinct peaks. Other reasons that could also have been a factor on this consistency were the focus of the subject and the unique features of individual subjects.

5.5.1. Focus

To clearly see a difference between EEGs of when a subject moves its hands or not, the subject needs to be only focused on moving its hands and not accidentally think of moving, for example, its feet or mouth. To further enhance the subject its focus, be place them at a quiet place not to be distracted by factors such as sudden noise. To help the subject retain focus and to effectively order the subject when to move their left, right or both hands, a stimulation video following method D or E explained in section 4.4 was made with Openvibe. Next to that, according to studies, brain activity in mental fatigue state might have differences between resting state and task state[19], which might impact someone its focus. An example of this is the difference between two magnitude plots of the same subject, following method section 4.4 where eventually 15 trials of left and right hand are lumped together in one dataset of 30 trials. As far as we knew, the same external factors (same environment, sitting position, same experiment time) are the same, except for its fatigue it felt during the recording.

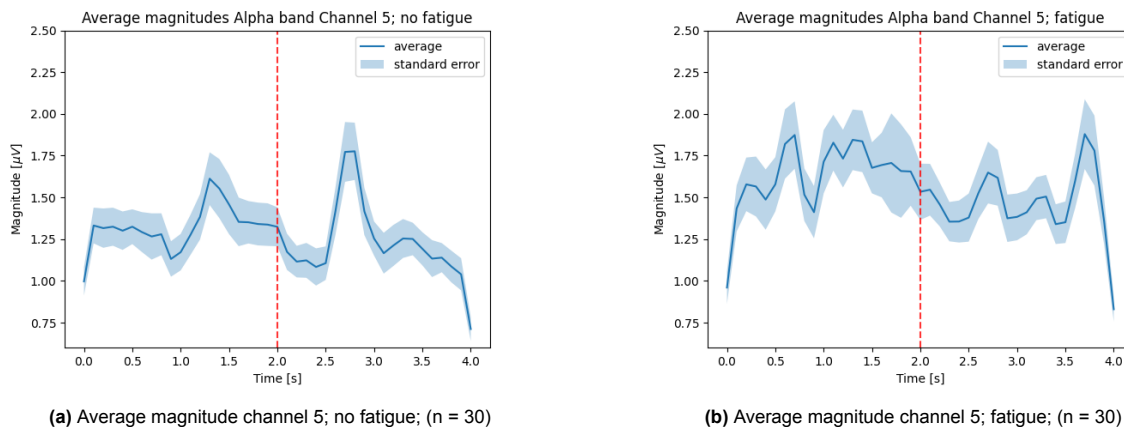


Figure 5.10: Magnitude plots of subject without (Figure 5.10a) or with (Figure 5.10b) fatigue. In the plot where the subject is not fatigued, a more distinct ERD and ERS can be seen compared to where the subject is fatigued. Suggesting that fatigue plays a role in the quality of the obtained data.

As can be seen, there is a clear difference in the response directly after the cue at $t = 2$. With no fatigue, the difference in strength of the signal compared to before the visual cue is marginally greater than the difference of it with fatigue. However, there is a chance that this difference might also have been induced by an external factor or an internal factor that we did not know during recording.

5.5.2. Subject differences

Another factor to take into account is that the top of the head of each subject is different. Especially hair density on the scalp plays a big factor in the quality of each recording. More hair on the scalp means that there is a higher chance the electrodes are unable to touch the scalp and cannot receive the faint EEG signals from the brain. Although the 'railing' indicator in the OpenBCI GUI was used to adjust the electrodes as best as possible to a subject's head, it still could not prevent measurement errors caused by the bad connection between a electrode and scalp. An example are the following plots ranged from male test subjects with long to short hair, obtained with the same method as the method to see whether fatigue has an impact on measurement.

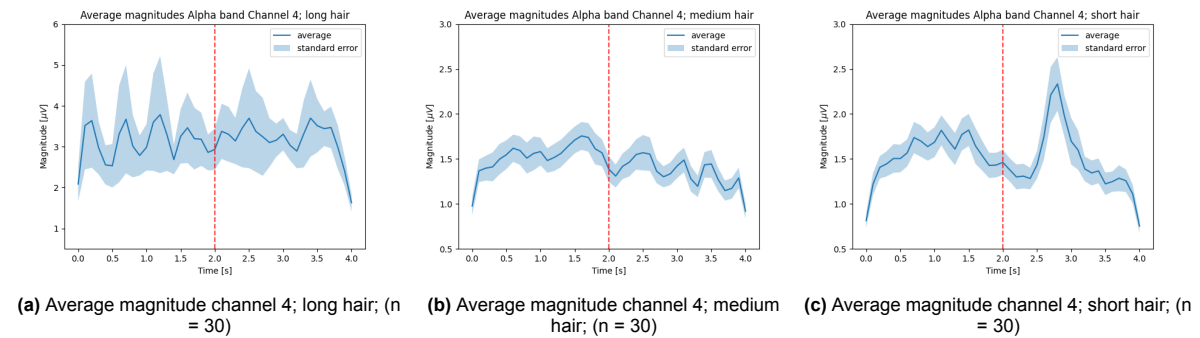


Figure 5.11: Magnitude plots of difference between subject with long hair (Figure 5.11a), medium long hair (Figure 5.11b) and short hair (Figure 5.11c). A clear increase in standard error can be seen between long hair and the other plots. Next to that, the medium long hair subject does not produce a distinct ERD or ERS where as the subject with short hair produces distinct ERD and ERS. These results suggest that the shorter the hair, the higher the chance for high quality data, but they might have also been influenced by the subject focus during recording.

Observe that the standard error and the average magnitude of the subject with long hair is much greater than the other two results. Leading to less reliable data. The subject with medium long hair produced lower standard error and average magnitude than the result with long hair, similar to the results of the subject with short hair. However, whereas the short haired subject produced a distinct peak after the cue, it could not be seen in the plot of the medium long haired subject. Still, this difference between medium long hair and short hair might have been impacted more by a difference in focus rather than a difference in hair length.

6

Conclusion and discussion

6.1. Conclusion

The goal of this subgroup was to see whether the chosen OpenBCI headset is able to see a difference between motor execution and the neutral state of a subject. Next to that, the recorded data is to be sent to the decoding group to decode them to actions.

Data acquisition

First a comparison, based on the set requirements, have been made between different headsets. Between the two available headsets, it was decided to use the OpenBCI headset instead of the Neurosky Mindwave, due to its amount of electrodes and flexibility of the placement of it. The detailed documentation from openBCI also played a role in this decision.

For the software, it was decided to use OpenVibe to extract data from the headset as this application supports different headsets and is specially made for the acquisition and processing of EEG signals. One of the requirements for the software was that it should be able to write recorded measurements to a csv file, which is a build-in function of Openvibe. One of the should-requirements for the application was it being able to live-stream data. OpenVibe supports different ways to stream data, one of the options is the in-built python box. Besides that, it is also possible to stream using TCP/IP. Unfortunately, the research on how to best integrate all components was not finished before the deadline of this thesis report.

Analysis

Using the OpenBCI headset and OpenVibe different experiments were done and analysed. To get rid of the DC component and the 50 Hz power line frequency a bandpass (7-30 Hz) and notch filter (48-52 Hz) were applied. It was found that these filters worked as intended, since their presence in the spectrogram were nullified.

It was found during experiments with blinking that if the subject blinks it can be clearly observed in the time-domain. This is due to the much higher amplitude of a blink in comparison the brain waves. The next step was to distinguish between neutral state (rest) and a motor task. It was found that this is not possible with only one measurement, but if the PSD of multiple measurements are averaged, a clear difference was seen. Namely, it was found that using the average PSD there is a higher power during movement compared to rest in most of the channels.

To see whether a change in magnitude occurs in time-domain during the exact moment a subject moves its hands, several trials were conducted. In the trials, the subject was instructed to follow a stimulation video where every 10 seconds a audio cue was given, followed by a visual cue with an arrow as indicator to move either their left or right hand. Merging the results from both left and right hand trials to create a magnitude- time plot, by comparing the magnitude of the extremes from zero seconds till two seconds after the cue with the average magnitude of before the cue, it was seen that the difference is around 1.4 - 1.6 times depending on the channel. This factor is around the set requirement, thus can be concluded that it is possible to distinguish between 2 classes, movement and rest. After that, the measurements were split again into separate trials of right and left hand. Using this and plotting the

magnitude plot again, it was found that it looks like it is possible to distinguish between left and right motor execution, due to the right hand having a slightly greater ERS/ERD response at the channel on the left hemisphere of the brain and vice versa for the left hand on the right hemisphere channel. However, due to the small difference in their respective responses, it cannot be said with certainty that the headset is able to differentiate between left handed and right handed motor execution. As a consequence the should-requirement for distinguish 3 classes is not met. One of the last requirements was the measuring of training data for the decode group. This was done using stimulation videos and at least 100 trials with four different subjects are made for this.

Quality improvement

Before doing the measurements different precautions were taken to improve the quality of the signal. This includes for example: unplugging of the laptop charger during measurements, not touching the laptop during measurements and sit at least 2 meter away from a power outlet. To further improve the quality of the signal, different methods were thought of, like grounding and blocking external electromagnetic waves with aluminium foil, re-referencing and determining the difference in interference between outside and inside to see if the headset is able to remove unwanted noise by its build-in common-mode noise rejection. After the measurement with a watermelon, which showed there was no difference in noise inside versus outside, it was concluded that the referencing and the CMR of the headset worked as intended. Due to this, the ideas of grounding a subject and wrapping aluminium foil around the headset were eventually dropped. As for the re-referencing, average referencing was tried, but yielded no improvement in signal quality.

6.2. Discussion

The result of the project sees promising. The analysis shows that it's possible to distinguish between 2 classes (movement and rest) in a plot of the average over different measurements. It was seen that if only one measurement is taken, the plots were not coherent enough to distinguish between the different classes.

During the project it was found that several factors are important for recording consistent measurements; namely focus and the differences between subjects. This was experienced by the fact that the data of the subject recorded on one day gives different results although the exact the same procedure was followed on another day. The subject has indicated that he was more tired on the second day, which could be a reason for the reduced quality in the data.

Besides that, it was experienced that recording consistent data, where a action takes place at the exact same time, is a requirement to effectively distinguish between classes. Using a stimulation video is thus recommended for future groups, as this will give the exact time of a stimulation even with the delay of the headset and ensures that the subject will execute a movement at the same time across multiple trials.

To extract the data from the headset in this project it was decided to use OpenVibe. OpenVibe shows to be an application that met all requirements that were set, such as being able to write data directly into a csv file. Next to that, its visual interface and broad library of different functions make it a attractive tool to use for EEG data acquisition and processing. One of the complications that was found during the project is the fact that integration of other codes, like Python, is difficult. Due to this difficulty the integration was not yet finished, but this can be continued by using the IP streaming function of OpenVibe.

Future work

While the presented project results comply with almost all requirements, there are a number of improvements that can be made in future projects:

- Due to time constrains it was in this project not possible to record measurements with motor imagery. This could be an opportunity for future groups to investigate if the same conclusions can be made using motor imagery. We would recommend to do as least 50 trials as this will decrease the standard error of the measurements.

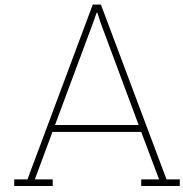
- More subjects should be found and more trials per subject should be conducted in general. With that, more data could be acquired and a more solid conclusion can be given about the functionality of the OpenBCI headset or another EEG headset.
- Different windows, window sizes and overlaps could be experimented with to discover what the best ratio of time-resolution and frequency-resolution for this project is.
- Too many paradigms were created in the beginning with most of them proving ineffective, next to that the importance of a stimulation video was underestimated to obtain constant data. A recommendation to following teams would be to start with the stimulation video from the very first measurement and stick to a maximum of 2 - 3 paradigms after intensive research of papers with a similar goal of obtaining motor execution and/or control data.
- The OpenBCI headset was not as comfortable and user friendly as hoped, due to the amount of trouble to adjust the electrodes for each subject. Each electrode has to be disconnected from the main board to prevent damage of the jumper cables and screwed further in or out to get the electrodes to touch the scalp. However, this screwing in and out of the electrodes could not be done while the headset worn by the subject, because their hair would get tangled in the pointy electrodes. A recommendation for a future project might be to experiment with another headset like the Emotiv Epoc, which does not have this mechanism of screw-in electrodes.

References

- [1] Priyanka A. Abhang, Bharti W. Gawali, and Suresh C. Mehrotra. "Chapter 2 - Technological Basics of EEG Recording and Operation of Apparatus". In: *Introduction to EEG- and Speech-Based Emotion Recognition*. Ed. by Priyanka A. Abhang, Bharti W. Gawali, and Suresh C. Mehrotra. Academic Press, 2016, pp. 19–50. ISBN: 978-0-12-804490-2. DOI: <https://doi.org/10.1016/B978-0-12-804490-2.00002-6>. URL: <https://www.sciencedirect.com/science/article/pii/B9780128044902000026>.
- [2] Mohit Agarwal and Raghupathy Sivakumar. "Blink: A Fully Automated Unsupervised Algorithm for Eye-Blink Detection in EEG Signals". In: *2019 57th Annual Allerton Conference on Communication, Control, and Computing (Allerton)*. IEEE, Sept. 2019. DOI: 10.1109/allerton.2019.8919795. URL: <https://doi.org/10.1109/allerton.2019.8919795>.
- [3] "Arousal effect on emotional face comprehension: Frequency band changes in different time intervals". In: *Physiology Behavior* 97.3 (2009), pp. 455–462. ISSN: 0031-9384. DOI: <https://doi.org/10.1016/j.physbeh.2009.03.023>. URL: <https://www.sciencedirect.com/science/article/pii/S0031938409001449>.
- [4] *BCI competition II dataset III*. URL: <https://www.bbci.de/competition/ii/>.
- [5] Xun Chen et al. "Removal of Muscle Artifacts From the EEG: A Review and Recommendations". In: *IEEE Sensors Journal* 19.14 (2019), pp. 5353–5368. DOI: 10.1109/JSEN.2019.2906572.
- [6] *Compliance Approved Bluetooth 4.0 Low Energy BLE RF Module With Built-In ARM Cortex M0 Microcontroller*. URL: <https://docs.rs-online.com/32f2/0900766b8138299e.pdf>.
- [7] Gianluca Di Flumeri et al. "The Dry Revolution: Evaluation of Three Different EEG Dry Electrode Types in Terms of Signal Spectral Features, Mental States Classification and Usability". In: *Sensors* 19.6 (Mar. 2019), p. 1365. DOI: 10.3390/s19061365. URL: <https://doi.org/10.3390/s19061365>.
- [8] Robert M. Hardwick et al. "Neural correlates of action: Comparing meta-analyses of imagery, observation, and execution". In: *Neuroscience & Biobehavioral Reviews* 94 (Nov. 2018), pp. 31–44. DOI: 10.1016/j.neubiorev.2018.08.003. URL: <https://doi.org/10.1016/j.neubiorev.2018.08.003>.
- [9] Mawia A Hassan and Elwathiq A Mahmoud. "A Comparison between Windowing FIR Filters for Extracting the EEG Components". In: *Journal of Biosensors & Bioelectronics* 06.04 (2015). DOI: 10.4172/2155-6210.1000191. URL: <https://doi.org/10.4172/2155-6210.1000191>.
- [10] Hermann Hinrichs et al. "Comparison between a wireless dry electrode EEG system with a conventional wired wet electrode EEG system for clinical applications". In: *Scientific Reports* 10.1 (Mar. 2020). DOI: 10.1038/s41598-020-62154-0. URL: <https://doi.org/10.1038/s41598-020-62154-0>.
- [11] Texas Instruments. *PIC32MX1XX/2XX 28/36/44-PIN*. ADS1299-xLow-Noise, 4-, 6-, 8-Channel, 24-Bit, Analog-to-Digital Converter for EEG and Biopotential Measurements. 2012, revised 2017.
- [12] Aditya Jain et al. "A comparative study of visual and auditory reaction times on the basis of gender and physical activity levels of medical first year students". In: *International Journal of Applied and Basic Medical Research* 5.2 (2015), p. 124. DOI: 10.4103/2229-516x.157168. URL: <https://doi.org/10.4103/2229-516x.157168>.
- [13] Manzoor Khazi, Atul Kumar, and MJ Vidya. "Analysis of EEG using 10: 20 electrode system". In: *International Journal of Innovative Research in Science, Engineering and Technology* 1.2 (2012), pp. 185–191.

- [14] Jyoti Singh Kirar and R. K. Agrawal. "Relevant Frequency Band Selection using Sequential Forward Feature Selection for Motor Imagery Brain Computer Interfaces". In: *2018 IEEE Symposium Series on Computational Intelligence (SSCI)*. 2018, pp. 52–59. DOI: 10.1109/SSCI.2018.8628719.
- [15] Fabian Klostermann et al. "Task-related differential dynamics of EEG alpha- and beta-band synchronization in cortico-basal motor structures". In: *European Journal of Neuroscience* 25.5 (Apr. 2007), pp. 1604–1615. DOI: 10.1111/j.1460-9568.2007.05417.x. URL: <https://doi.org/10.1111/j.1460-9568.2007.05417.x>.
- [16] John LaRocco, Minh Dong Le, and Dong-Guk Paeng. "A Systemic Review of Available Low-Cost EEG Headsets Used for Drowsiness Detection". In: *Frontiers in Neuroinformatics* 14 (Oct. 2020). DOI: 10.3389/fninf.2020.553352. URL: <https://doi.org/10.3389/fninf.2020.553352>.
- [17] LDS. "Understanding FFT Windows". In: (). URL: https://www.egr.msu.edu/classes/me451/me451_labs/Fall_2013/Understanding_FFT_Windows.pdf.
- [18] Min-Ho Lee et al. "EEG dataset and OpenBMI toolbox for three BCI paradigms: an investigation into BCI illiteracy". In: *GigaScience* 8.5 (Jan. 2019). DOI: 10.1093/gigascience/giz002. URL: <https://doi.org/10.1093/gigascience/giz002>.
- [19] Gang Li et al. "The impact of mental fatigue on brain activity: a comparative study both in resting state and task state using EEG". In: *BMC Neuroscience* 21.1 (May 2020). DOI: 10.1186/s12868-020-00569-1. URL: <https://doi.org/10.1186/s12868-020-00569-1>.
- [20] Jussi Lindgren and Anatole Lecuyer. "OpenViBE and Other BCI Software Platforms". In: *Brain-Computer Interfaces 2*. John Wiley & Sons, Inc., Sept. 2016, pp. 179–198. DOI: 10.1002/9781119332428.ch10. URL: <https://doi.org/10.1002/9781119332428.ch10>.
- [21] Microchip. *PIC32MX1XX/2XX 28/36/44-PIN*. <https://www.microchip.com/en-us/product/pic32mx250f128b#>. 2011-2019.
- [22] Luis Fernando Nicolas-Alonso and Jaime Gomez-Gil. "Brain Computer Interfaces, a Review". In: *Sensors* 12.2 (Jan. 2012), pp. 1211–1279. DOI: 10.3390/s120201211. URL: <https://doi.org/10.3390/s120201211>.
- [23] César Noronha. *Choosing your reference for an EEG recording and the advantage of use Analyzer*. 2019. URL: <https://www.brainlatam.com/blog/choosing-your-reference-for-an-eeeg-recording-and-the-advantage-of-use-analyzer-696>.
- [24] Olugbemi T. Olaniyan et al. "Neural signaling and communication using machine learning". In: *Artificial Intelligence for Neurological Disorders*. Elsevier, 2023, pp. 245–260. DOI: 10.1016/b978-0-323-90277-9.00010-9. URL: <https://doi.org/10.1016/b978-0-323-90277-9.00010-9>.
- [25] OpenBCI. *Cyton Data Format*. 2021. URL: <https://docs.openbci.com/Cyton/CytonDataFormat/>.
- [26] Natasha Padfield et al. "EEG-Based Brain-Computer Interfaces Using Motor-Imagery: Techniques and Challenges". In: *Sensors* 19.6 (Mar. 2019), p. 1423. DOI: 10.3390/s19061423. URL: <https://doi.org/10.3390/s19061423>.
- [27] G. Pfurtscheller and F.H. Lopes da Silva. "Event-related EEG/MEG synchronization and desynchronization: basic principles". In: *Clinical Neurophysiology* 110.11 (1999), pp. 1842–1857. ISSN: 1388-2457. DOI: [https://doi.org/10.1016/S1388-2457\(99\)00141-8](https://doi.org/10.1016/S1388-2457(99)00141-8). URL: <https://www.sciencedirect.com/science/article/pii/S1388245799001418>.
- [28] G. Pfurtscheller and C. Neuper. "Motor imagery and direct brain-computer communication". In: *Proceedings of the IEEE* 89.7 (2001), pp. 1123–1134. DOI: 10.1109/5.939829.
- [29] G. Pfurtscheller et al. "Mu rhythm (de)synchronization and EEG single-trial classification of different motor imagery tasks". In: *NeuroImage* 31.1 (2006), pp. 153–159. ISSN: 1053-8119. DOI: <https://doi.org/10.1016/j.neuroimage.2005.12.003>. URL: <https://www.sciencedirect.com/science/article/pii/S1053811905025140>.

- [30] Yann Renard et al. "OpenViBE: An Open-Source Software Platform to Design, Test, and Use Brain–Computer Interfaces in Real and Virtual Environments". In: *Presence: Teleoperators and Virtual Environments* 19.1 (Feb. 2010), pp. 35–53. DOI: 10.1162/pres.19.1.35. URL: <https://doi.org/10.1162/pres.19.1.35>.
- [31] Lin Tao et al. "Distribution Adaptation and Classification Framework Based on Multiple Kernel Learning for Motor Imagery BCI Illiteracy". In: *Sensors* 22.17 (Aug. 2022), p. 6572. DOI: 10.3390/s22176572. URL: <https://doi.org/10.3390/s22176572>.
- [32] Dezhong Yao. "Is the Surface Potential Integral of a Dipole in a Volume Conductor Always Zero? A Cloud Over the Average Reference of EEG and ERP". In: *Brain Topography* 30.2 (Feb. 2017), pp. 161–171. DOI: 10.1007/s10548-016-0543-x. URL: <https://doi.org/10.1007/s10548-016-0543-x>.
- [33] Dezhong Yao et al. "Which Reference Should We Use for EEG and ERP practice?" In: *Brain Topography* 32.4 (Apr. 2019), pp. 530–549. DOI: 10.1007/s10548-019-00707-x. URL: <https://doi.org/10.1007/s10548-019-00707-x>.
- [34] Zhiwen Zhang et al. "A Novel Deep Learning Approach With Data Augmentation to Classify Motor Imagery Signals". In: *IEEE Access* 7 (2019), pp. 15945–15954. DOI: 10.1109/ACCESS.2019.2895133.



Additional figures hardware overview

A.1. OpenBCI electrodes



(a) Spikey electrodes



(b) Non spikey electrodes



(c) Comfort units

Figure A.1: Different kind of electrodes available for the OpenBCI headset

B

Additional figures data acquisition

B.1. Brain structure

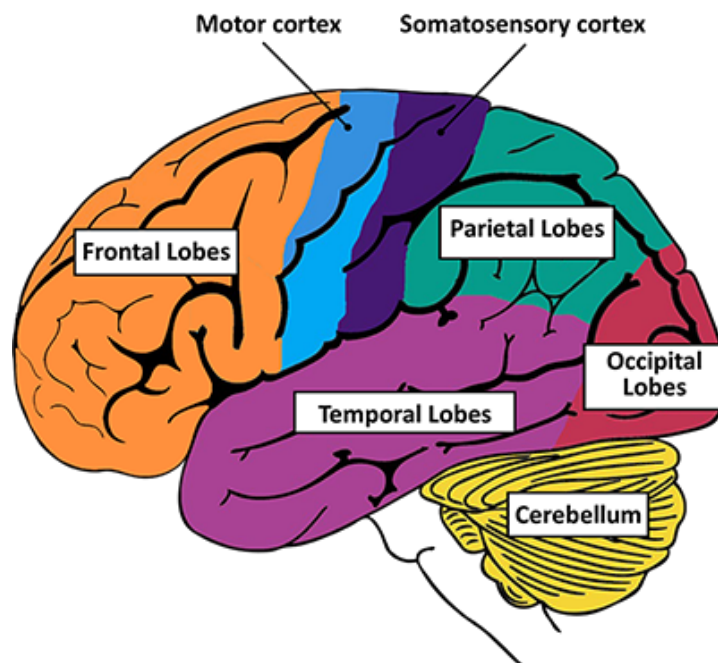


Figure B.1: Brain structure ¹

¹<https://www.ninds.nih.gov/health-information/public-education/brain-basics/brain-basics-know-your-brain>

B.2. Overview methodologies

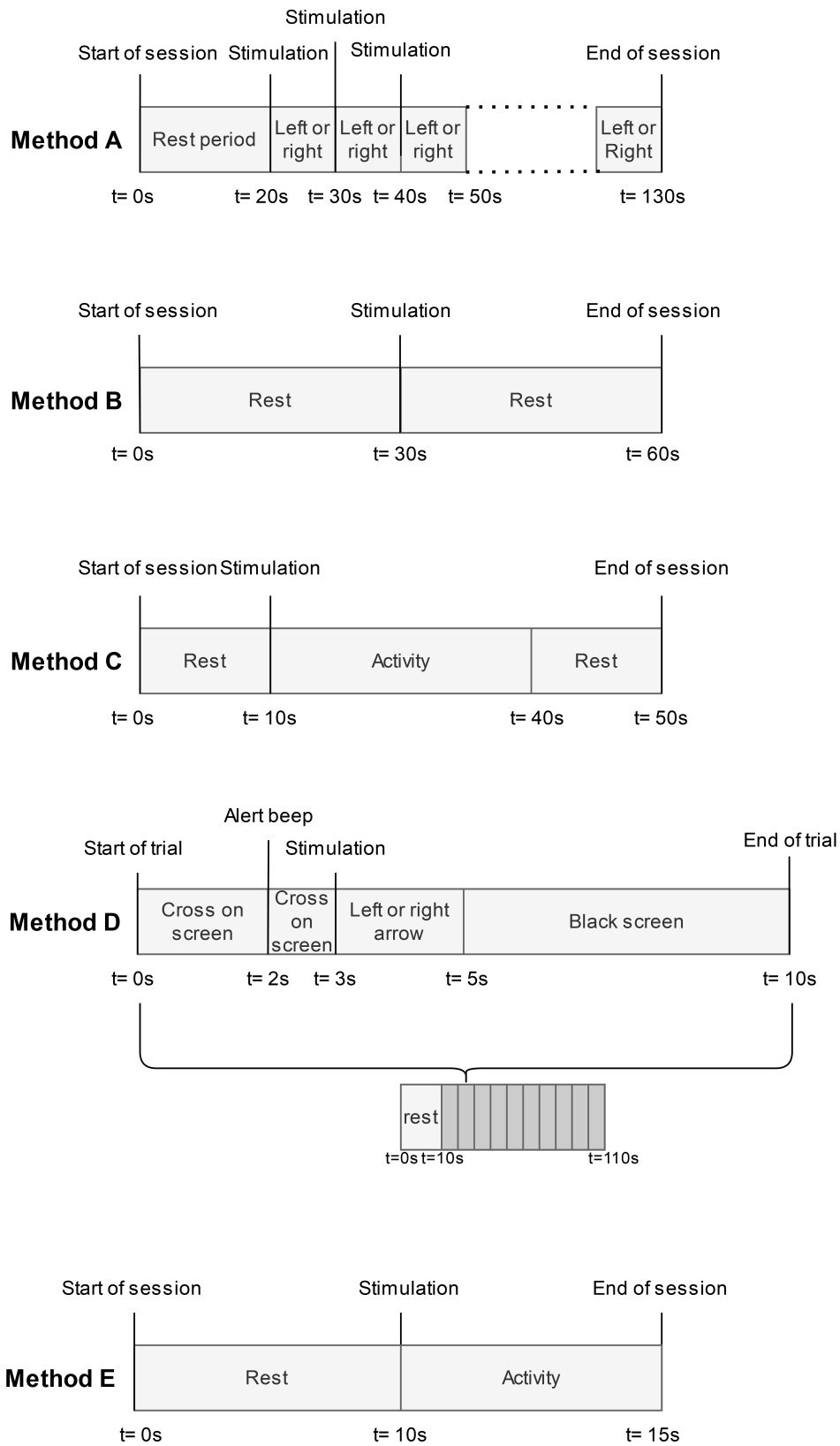


Figure B.2: An overview of the methodology of the used methods

B.3. OpenVibe scenario

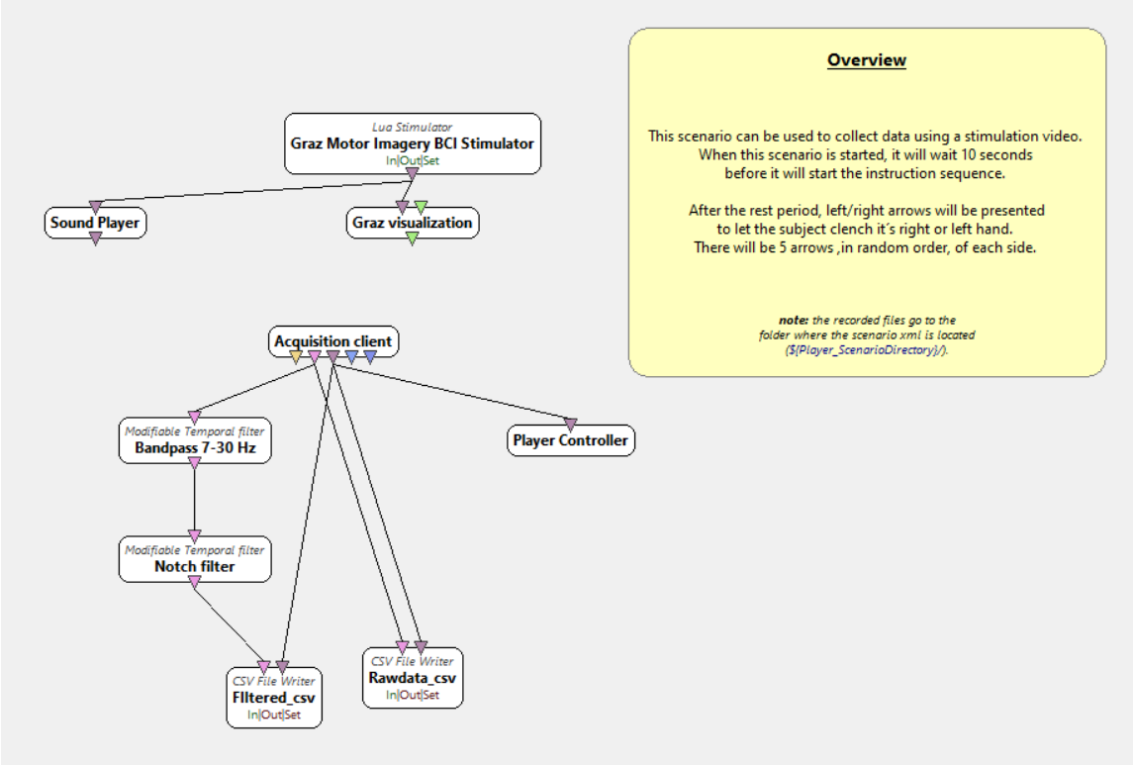
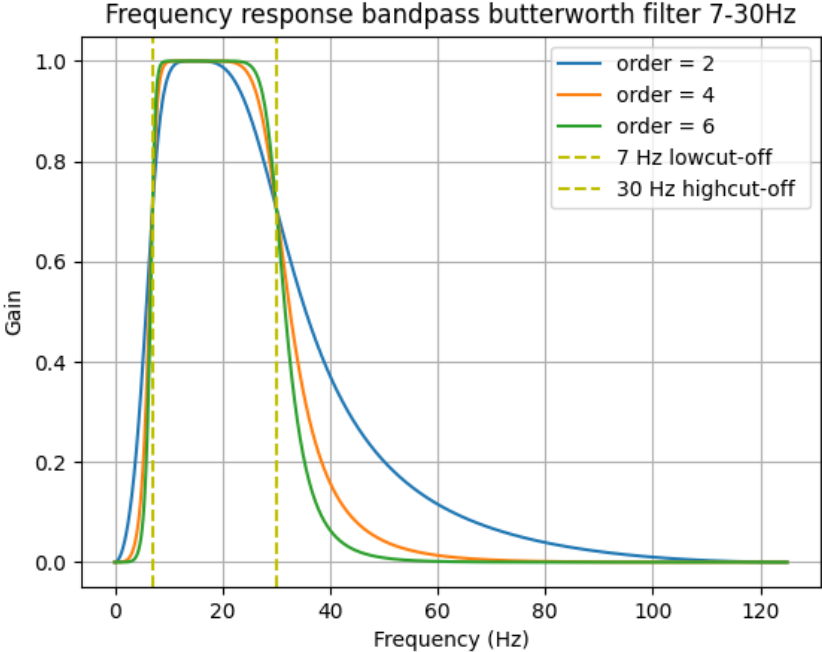
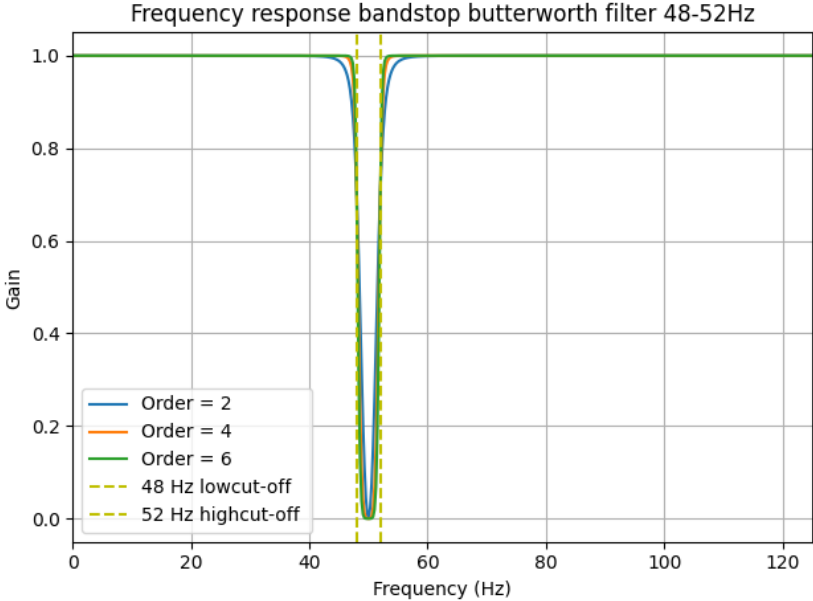


Figure B.3: A scenario in OpenVibe which will be used regularly during the project

B.4. Pre-processing filters



(a) Frequency response butterworth bandpass filter from 7 till 30 Hz for different orders



(b) Frequency response butterworth bandstop filter from 48 till 52 Hz for different orders

Figure B.4: Frequency responses for the used pre-processing filters

B.5. OpenBCI GUI

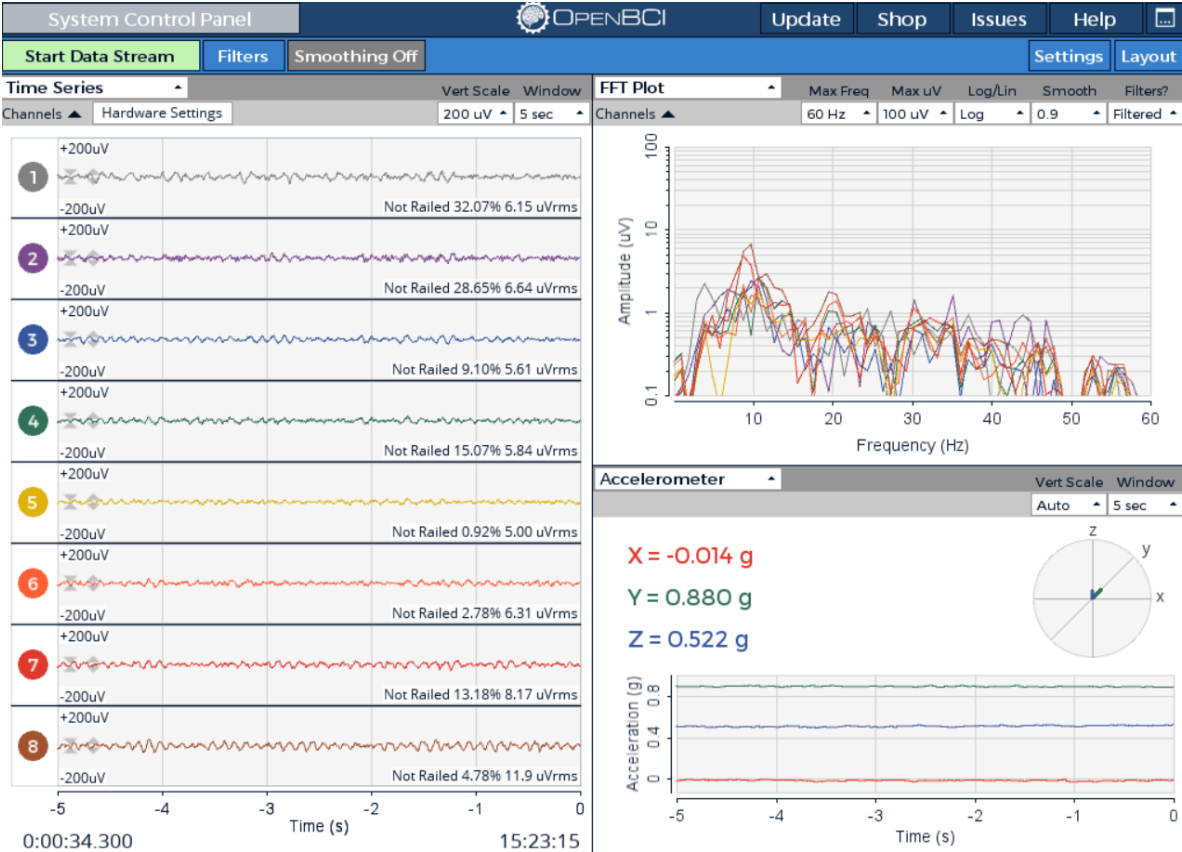


Figure B.5: An example of alpha waves using the OpenBCI GUI

C

Additional figures data analysis

C.1. Raw signal

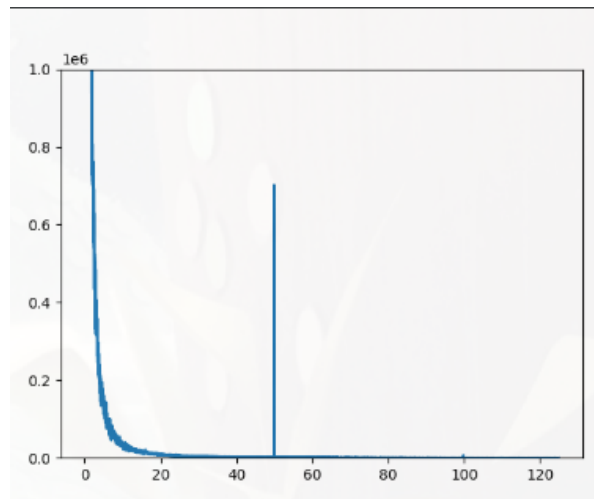


Figure C.1: Raw signal fft plot

C.2. PSD plots

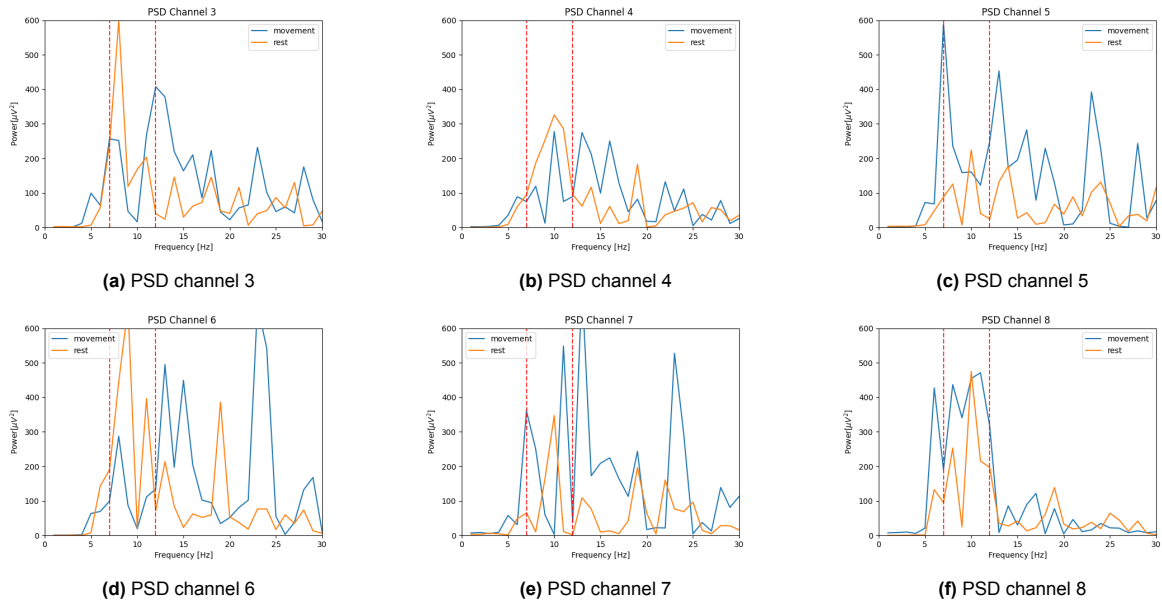


Figure C.2: PSDs movement vs rest of channels 3 - 8

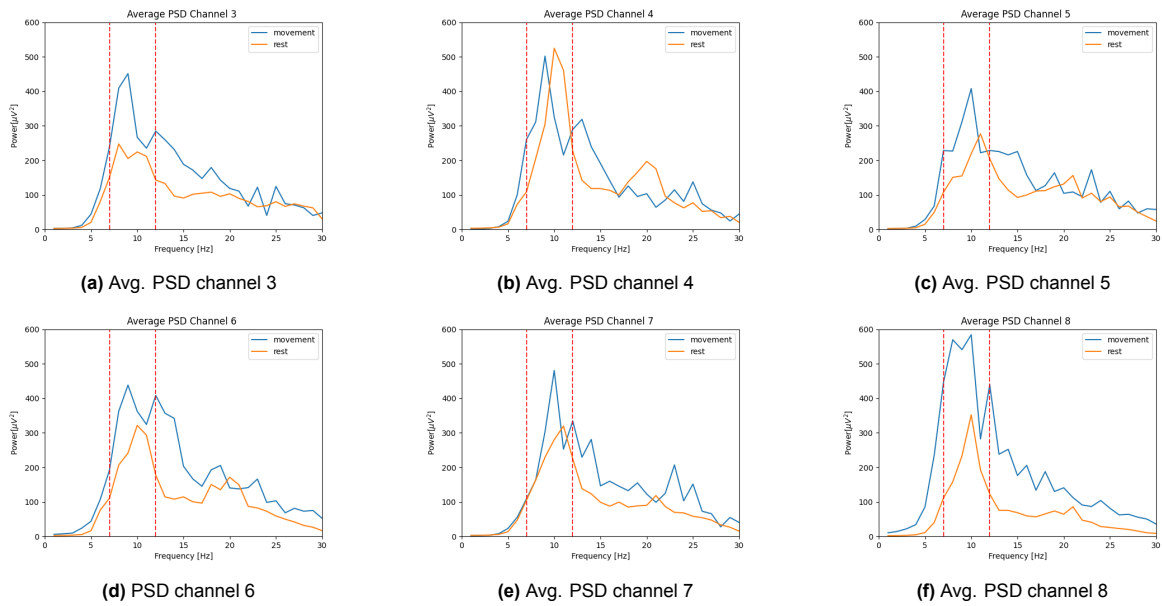


Figure C.3: Avg. PSDs movement vs rest of channels 3 - 8

C.3. Window sizes

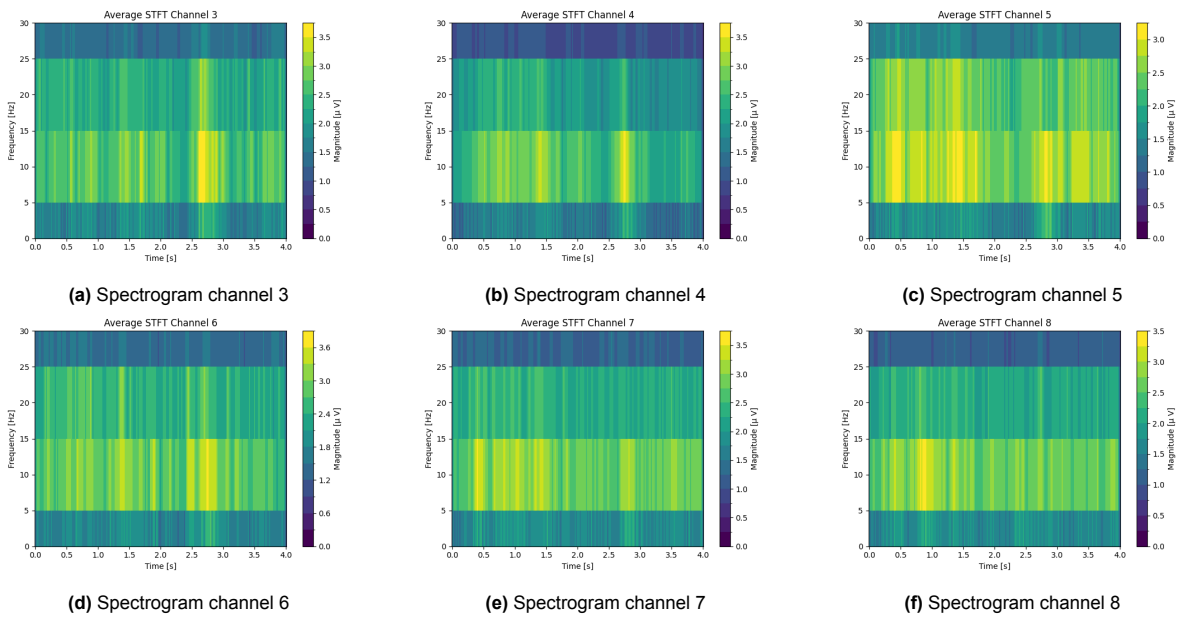


Figure C.4: Avg. Spectrogram channel 3 - 8; 0.1 second Hann window

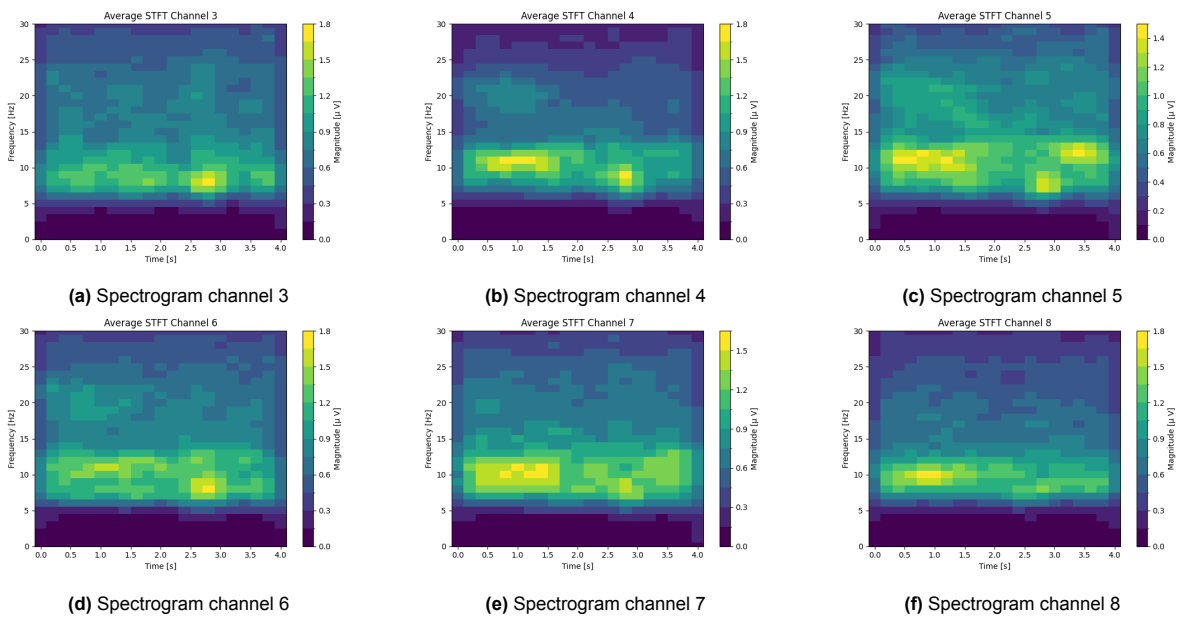


Figure C.5: Avg. Spectrogram channel 3 - 8; 1 second Hann window

C.4. Average magnitude plots

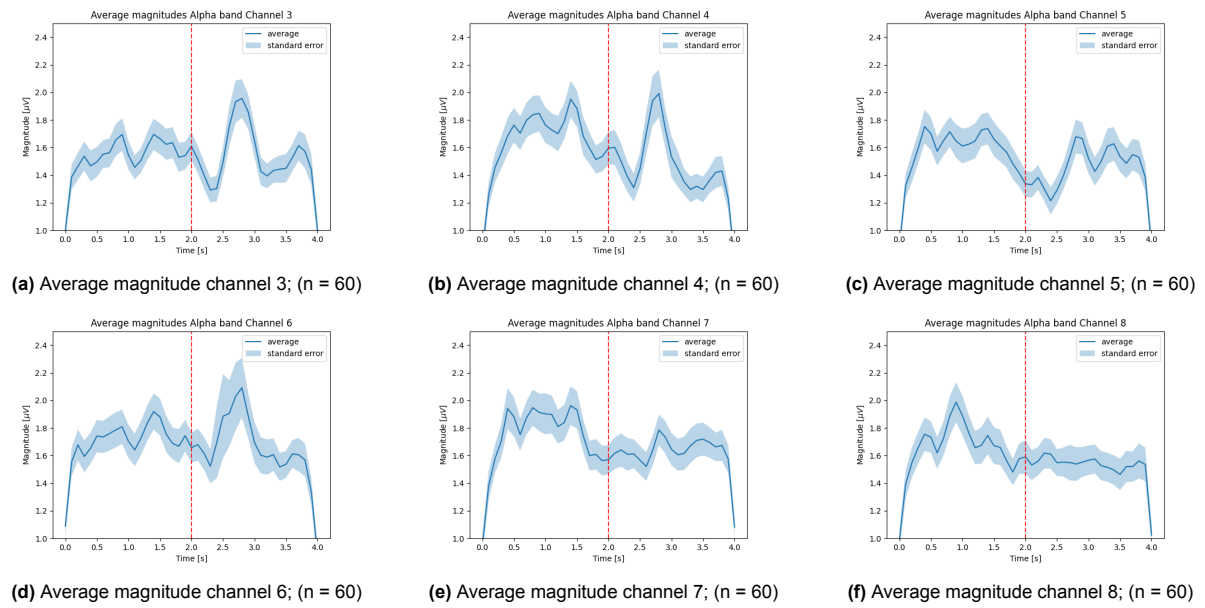


Figure C.6: Avg. magnitude of channels 3 - 8 in Alpha band (7 - 12 Hz)

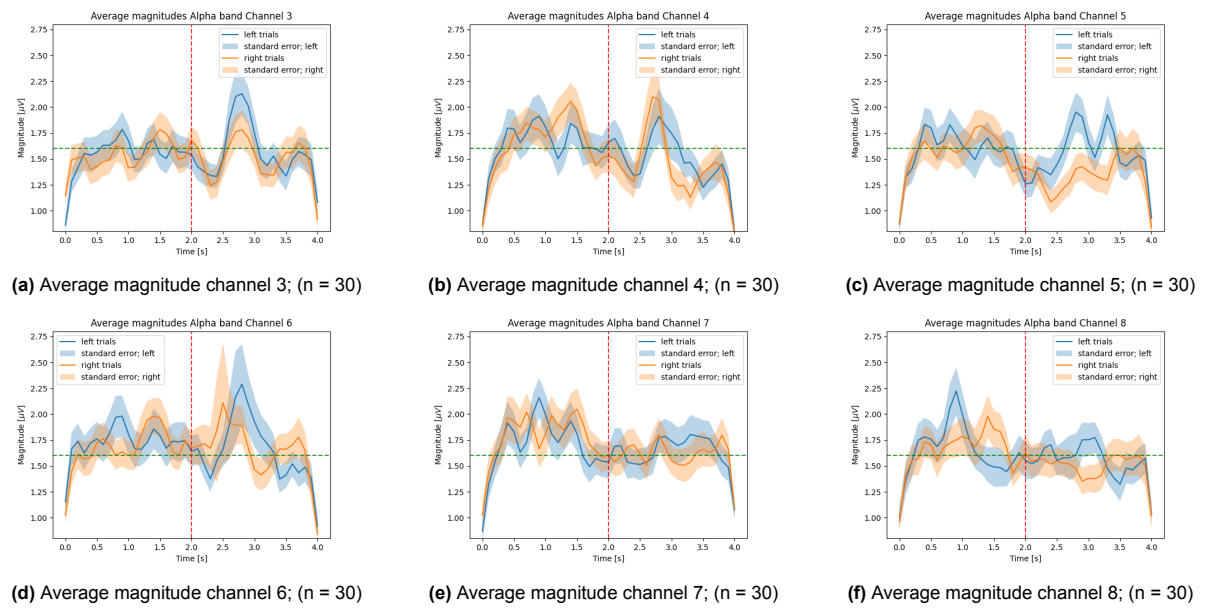


Figure C.7: Avg. magnitude of channels 3 - 8 in Alpha band (7 - 12 Hz) between left and right trials

C.5. Beta band magnitude plots

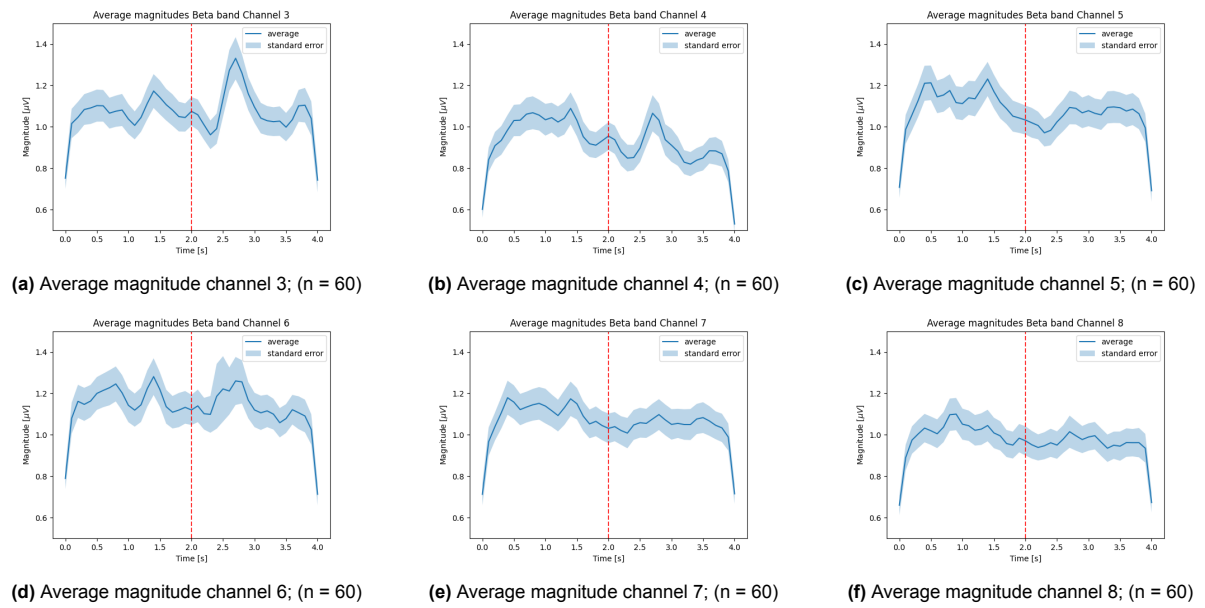


Figure C.8: Avg. magnitude of channels 3 - 8 in Beta band (12 - 30 Hz)

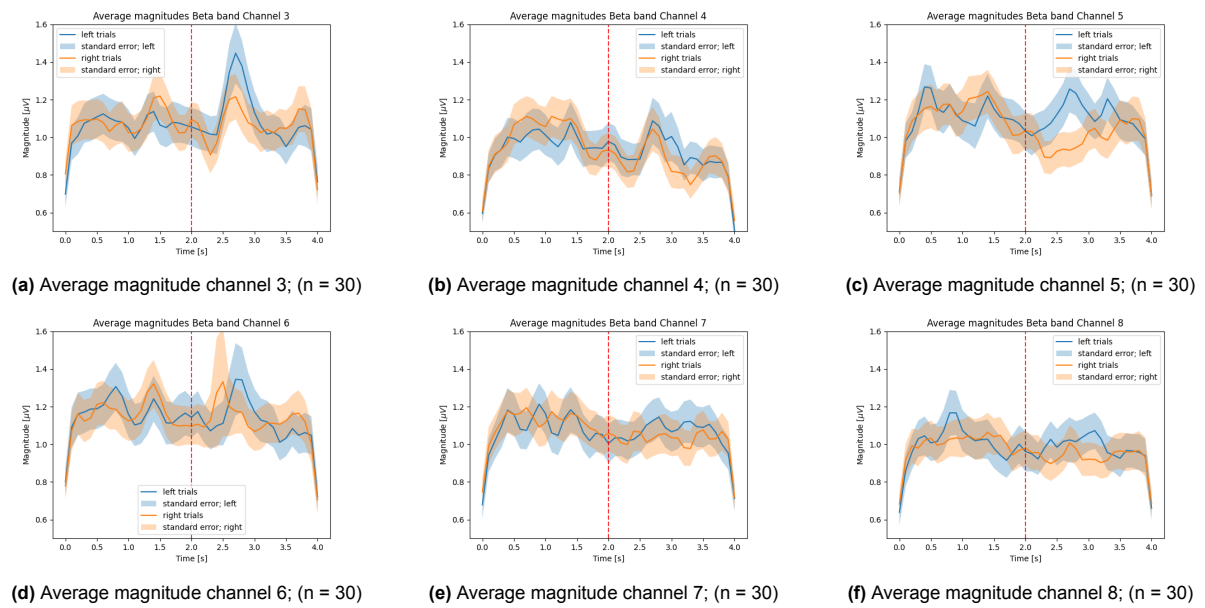


Figure C.9: Avg. magnitude of channels 3 - 8 in Beta band (12 - 30 Hz) between left and right trials

C.6. Quality improvement

C.6.1. Human antenna

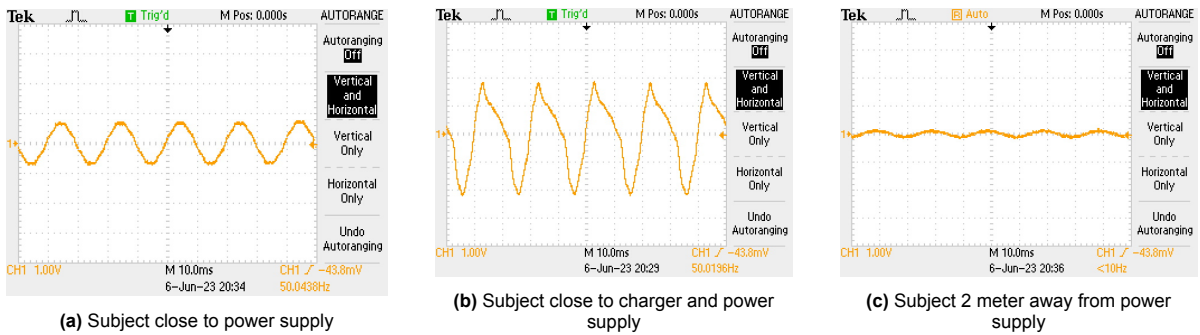


Figure C.10: Different experiment measuring voltage over time interference from power supply

C.6.2. Noise reduction

Grounding

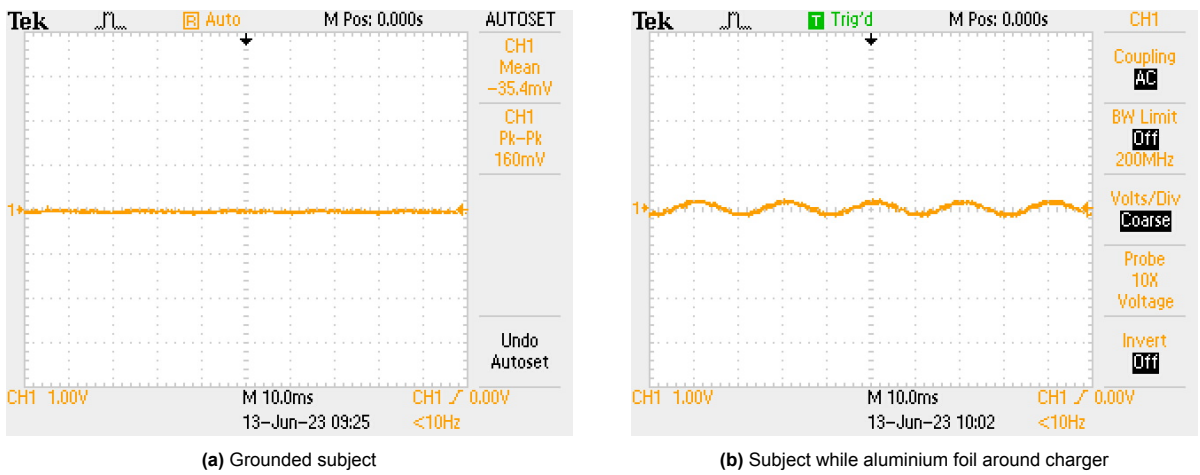


Figure C.11: Ground and aluminium foil to potentially reduce noise

inside vs outside

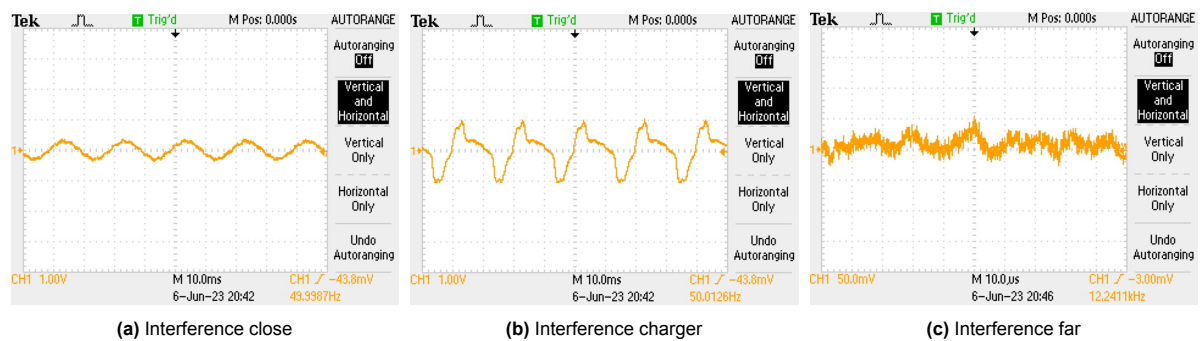
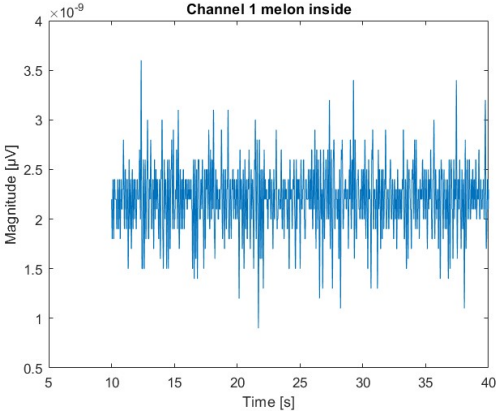
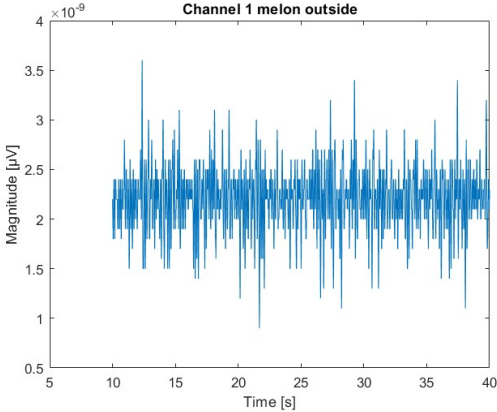


Figure C.12: Interference shown on oscilloscope of melon

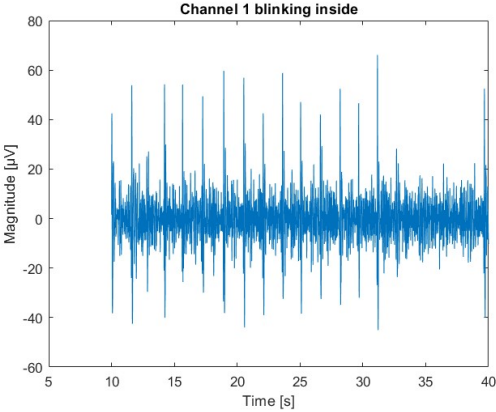


(a) Time domain plot melon measured inside

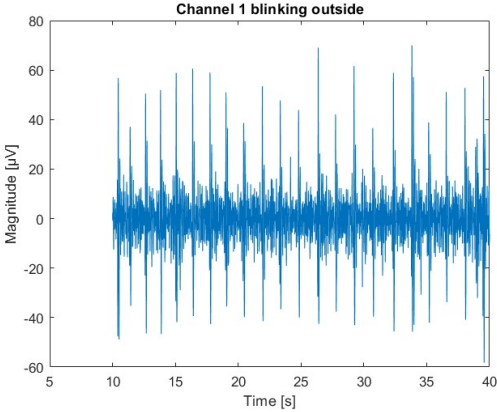


(b) Time domain plot melon measured outside

Figure C.13: Time domain plot watermelon inside and outside



(a) Time domain plot blinking measured inside



(b) Time domain plot blinking measured outside

Figure C.14: Time domain plot blinking inside and outside